

---

Masters Theses

Student Theses and Dissertations

---

1967

## Mass transfer from a torus shaped body

Kamalesh Suryakant Desai

Follow this and additional works at: [https://scholarsmine.mst.edu/masters\\_theses](https://scholarsmine.mst.edu/masters_theses)

 Part of the [Chemical Engineering Commons](#)

Department:

---

### Recommended Citation

Desai, Kamalesh Suryakant, "Mass transfer from a torus shaped body" (1967). *Masters Theses*. 5160.  
[https://scholarsmine.mst.edu/masters\\_theses/5160](https://scholarsmine.mst.edu/masters_theses/5160)

This thesis is brought to you by Scholars' Mine, a service of the Missouri S&T Library and Learning Resources. This work is protected by U. S. Copyright Law. Unauthorized use including reproduction for redistribution requires the permission of the copyright holder. For more information, please contact [scholarsmine@mst.edu](mailto:scholarsmine@mst.edu).

MASS TRANSFER FROM  
A TORUS SHAPED BODY

BY

KAMALESH SURYAKANT DESAI - 1944

---

A

THESIS

submitted to the faculty of

THE UNIVERSITY OF MISSOURI AT ROLLA

in partial fulfillment of the requirements for the

Degree of

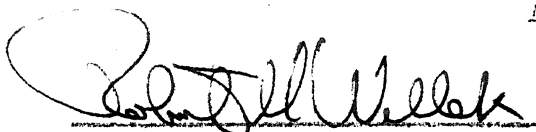

MASTER OF SCIENCE IN CHEMICAL ENGINEERING

Rolla, Missouri

1967

---

Approved by

 (advisor) 

---



---

## TABLE OF CONTENTS

	Page
ACKNOWLEDGEMENT . . . . .	iv
LIST OF FIGURES . . . . .	v
LIST OF TABLES . . . . .	vi
NOMENCLATURE . . . . .	vii
ABSTRACT . . . . .	x
I. INTRODUCTION . . . . .	1
II. LITERATURE REVIEW . . . . .	5
Mass Transfer Mechanisms . . . . .	5
Newman Model . . . . .	5
Kronig and Brink Model . . . . .	6
Rose and Kintner Model . . . . .	7
Surface Stretch Model . . . . .	10
Handlos and Baron Model . . . . .	13
III MATHEMATICAL MODEL . . . . .	18
Diffusion Equation . . . . .	18
A Coordinate Transformation . . . . .	21
IV. THE SOLUTION . . . . .	23
The Method of Solution . . . . .	23
Classical Explicit Method . . . . .	25
Finite Difference Equations . . . . .	26
Volumetric Average Concentration . . . . .	30
Analytical Solution For A Cylinder . . . . .	31
Computational Error . . . . .	31
Stability . . . . .	32

	Page
V. RESULTS AND DISCUSSION . . . . .	34
Point Concentrations . . . . .	34
Fraction Extracted . . . . .	36
Effect of Mesh Size on Numerical Solution . . . . .	37
Analytical Solution For A Cylinder . .	37
VI. CONCLUSION . . . . .	52
VII. APPENDICES . . . . .	54
A. Diffusion Equation . . . . .	55
B. Numerical Solution of Equation (4.21) . . . . .	56
C. Analytical Solution for a Cylinder . . . . .	57
D. Truncation Error . . . . .	61
E. Computer Program for the Numerical Solution . . . . .	63
VIII. BIBLIOGRAPHY . . . . .	70
IX. VITA . . . . .	71

## ACKNOWLEDGEMENT

The author is grateful to Dr. R. M. Wellek, Associate Professor of Chemical Engineering, who suggested this investigation and served as a research advisor. His help, guidance and encouragement are sincerely appreciated. The author is also grateful to the following: (1) Computer Science Center of the University of Missouri at Rolla for the computer time; (2) Dr. J. L. Rivers for his suggestions in framing an orthogonal toroidal coordinate system for the torus; (3) Mr. W. V. Andoe, for the discussion of the finite difference technique used to solve the partial differential equation consisting of three independent variables.

## LIST OF FIGURES

Figures		Page
1.A	Toroidal Bubble	3
1.B	Break-up of a Toroid	3
2.1	One Period of Mass Transfer Model	8
2.2	Handlos and Baron Stream Lines	15
3.1	A Part of the Torus	20
4.1	Net Work	24
4.2	Three Dimensional Explicit Method Pattern	27
5.1	Fraction Extracted Versus Dimensionless Time	48
5.2	Dimensionless Concentration At $X = -0.8$ Versus Dimensionless Time	49
5.3	Dimensionless Concentration At $X = +0.8$ Versus Dimensionless Time	50
5.4	Part of the Cross Section of the Torus	51
E.1	Network for Symbols Used in the Computer Program	66

## LIST OF TABLES

Table		Page
5.1	Dissymmetry of the Concentration Profile ( $A = 1$ , $\Delta\zeta = 0.0005$ , $\Delta X = 0.05$ )	38
5.2	Dissymmetry of the Concentration Profile ( $A = 2$ , $\Delta\zeta = 0.0005$ , $\Delta X = 0.05$ )	39
5.3	Dissymmetry of the Concentration Profile ( $A = 4$ , $\Delta\zeta = 0.0005$ , $\Delta X = 0.05$ )	40
5.4	Analytical and Numerical Solution for a Cylinder	41
5.5	Dissymmetry of the Concentration Profile ( $A = 1$ , $\Delta\zeta = 0.0003$ , $\Delta X = 0.04$ )	42
5.6	Dissymmetry of the Concentration Profile ( $A = 2$ , $\Delta\zeta = 0.0003$ , $\Delta X = 0.04$ )	43
5.7	Dissymmetry of the Concentration Profile ( $A = 4$ , $\Delta\zeta = 0.0003$ , $\Delta X = 0.04$ )	44
5.8	Difference in the Dimensionless Concentration at $X = \pm 0.8$	45
5.9	Fraction Extracted for a Torus and a Cylinder	46
5.10	Concentration at the Center of the Torus	47

## NOMENCLATURE

- $A = a/r_1$ , dimensionless.  
 $a =$  distance of the circle from the center of the torus, (cm).  
 $a =$  radius or half axis length, (cm).  
 $a_0 =$  initial radius or half axis length, (cm).  
 $B_n =$  coefficient in series solution, dimensionless  
 $b =$  a constant defined by equation (2.10).  
 $C =$  Dimensionless concentration of the solute.  
 $C^* =$  equilibrium concentration (g. mole/liter)  
 $C_A =$  concentration of solute A.  
 $C_{A0} =$  initial concentration of solute A.  
 $C_{Af} =$  final concentration of solute A.  
 $C_c =$  continuous phase  
 $C_{i,j,k} =$  concentration at the point (X,Z) and time , (g. mole/liter).  
 $\bar{C}(\gamma) =$  volumetric average concentration, dimensionless  
 $D =$  diffusivity, (cm<sup>2</sup>/sec).  
 $D_L =$  molecular diffusivity of the solute in the dispersed phase, (cm<sup>2</sup>/sec).  
 $D_E =$  effective diffusivity  
 $D_{AB} =$  diffusivity of A in B.  
 $d =$  diameter of the droplet, (cm).  
 $E =$  fraction extracted =  $(C_{A0} - C_{Af}) / (C_{A0} - C_A)$   
 $\bar{E} =$  effective diffusivity predicted by equation (2.35), (cm<sup>2</sup>/sec).  
 $E_m =$  fraction extracted =  $1 - \bar{C}(\gamma)$   
 $i =$  number corresponding to X axis  
 $j =$  number corresponding to Z axis



$J_{Ay}$  = mass flux of species A relative to mass average velocity, (gm cm<sup>2</sup>/sec).

$K_D$  = overall mass transfer coefficient, (cm/sec).

$K$  = dimensionless mass transfer coefficient.

$k_d$  = dispersed phase mass transfer coefficient.

$k_0$  = instantaneous local mass transfer coefficient at a given time and position on the interface.

$n$  = mode of oscillation or index.

$\underline{n}$  = integer

$n_A$  = mass flux, (gm/cm<sup>2</sup>sec).

$R = \frac{r}{r_1}$  = dimensionless radius.

$\underline{r} = \frac{4r}{d}$  = dimensionless radius of the torus.

$r$  = radius of the torus, cylinder or sphere, (cm).

$r_1$  = maximum radius of the torus, (cm).

$r_A$  = reaction rate, (gm/cm<sup>3</sup> sec).

$S = \Delta\tau / (\Delta X)^2$

$S$  = area of time dependent surface, (cm<sup>2</sup>).

$S_0$  = characteristic reference area for constant surface, (cm<sup>2</sup>).

$t$  = time, (sec)

$t$  = time during free fall period

$\bar{t}$  = average circulation time in droplet

$t_0$  = characteristic constant for particular system considered.

$U$  = droplet free fall ( or rise ) velocity, (cm/sec).

$V$  = mass average velocity, (cm/sec).

$V_y$  = Y component of mass average velocity normal to the boundary for a moving surfact element, (cm/sec).

$W_A$  = mass fraction.

$X$  = dimensionless x distance.

$X$  = film thickness, (cm).

$X_0$  = initial film thickness.

$Y$  = coordinate axis

$Y$  = distance measured from the interface into the phase of interest.

$Z$  = dimensionless  $z$  distance

$z$  = coordinate axis

### Greek Letters

$\Delta X$  = step size in  $X$  direction.

$\Delta Z$  = step size in  $Z$  direction.

$\rho_s$  = mass concentration of the solute, ( $\text{gm}/\text{cm}^3$ ).

$\mu_d, \mu_c$  = viscosity of dispersed phase and continuous phase respectively, centipoise.

$\tau$  = dimensionless time variable defined by equation (3.18).

$\xi$  = torus radius, dimensionless.

$\lambda_n$  = eigen value.

$\alpha$  = parameter in equation (2.15), defined by equation (2.16).

$\alpha_n$  = defined by equation (C.3).

$\beta_n$  = defined by equation (C.4).

$\omega, \omega'$  = frequency and modified frequency of oscillation, (radians/sec).

$\sigma$  = interfacial tension, dynes/cm.

$\epsilon$  = dimensionless amplitude factor.

ABSTRACT

A mathematical model for molecular diffusion in a torus was derived. Handlos and Baron have assumed a system of tori in their eddy diffusion model for liquid-liquid extraction from droplets. However, the effect of torus curvature was neglected in their studies, since they assumed the torus could be represented by an infinite cylinder. In this study, the effect of torus curvature was considered on the concentration profile and the fraction of the solute extracted. The partial differential equation describing the model consists of three independent variables, and a finite difference technique was employed for the solution of the mathematical model.

It was found in this work that the concentration profiles within a torus differed from those in an infinite cylinder. However, it was also found that the fraction of solute extracted in a torus was nearly identical to that predicted using the solution for an infinite cylinder. Since the effect of the torus curvature is negligible, the solution for an infinite cylinder may be used for diffusion to a torus.

## I. INTRODUCTION

A dispersed phase of liquid droplets or gas bubbles is present in many types of liquid contactors. One of the major design problems is to predict the rate of mass transfer to (or from) the dispersed phase. Many mathematical models have been proposed for predicting the dispersed phase mass transfer coefficient for internally stagnant, circulating and/or oscillating droplets. These are reviewed in chapter II.

The Handlos and Baron model (4) is based on the assumption that internal circulation is fully developed. The circulation pattern within the spherical droplet is assumed to be a system of tori (see Figure 2.2). Handlos and Baron derived their eddy diffusion model in cylindrical coordinates assuming an infinite cylinder for the system of tori. Thus they neglected the effect of the curvature of torus.

The purpose of this investigation is to consider the effect of the torus curvature on the rate of mass (or heat) transfer in a torus. The eddy diffusivity term of the Handlos and Baron model was originally derived for radial diffusion only (i.e., the eddy diffusivity term was derived without considering the effect of torus curvature). Thus this term cannot be incorporated in the diffusion equation when the effect of torus curvature is considered. In this work only molecular

diffusion in the torus is studied, since the molecular diffusivity in normal liquids and gases is not a function of the direction of mass transfer. It is believed that the study of the molecular diffusion process will give some insight into the eddy diffusion model of Handlos and Baron.

It is also of interest to note that toroidal shaped bubbles (9) occasionally form at gas orifices submerged in a liquid (see Figure 1.A and 1.B which are reproduced here from the work of Rennie and Smith (9)). It is thus possible that the diffusion process in these bubbles could be described by the mathematical torus model to be developed in this work.

The molecular diffusion equation in differential form for a torus coordinate system is not reported in the literature. Therefore it is derived here. The unidirectional diffusion equations for a simple geometry such as plane sheet, a cylinder and a sphere are generally easily solved by analytic methods of mathematical physics. Completely analytical solutions are not reported in the literature for many complex three dimensional problems, because the differential equation is either not completely separable or it is highly nonlinear. In this work, the diffusion equation for the torus is solved numerically by a finite difference technique to obtain the concentration profile, the average concentration and the fraction

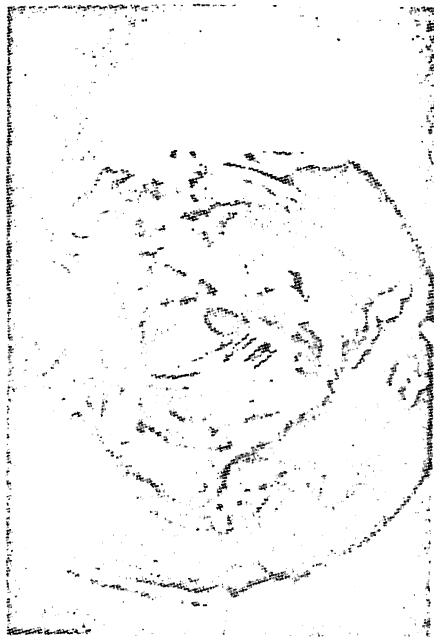


Figure 1.A  
Toroidal bubble

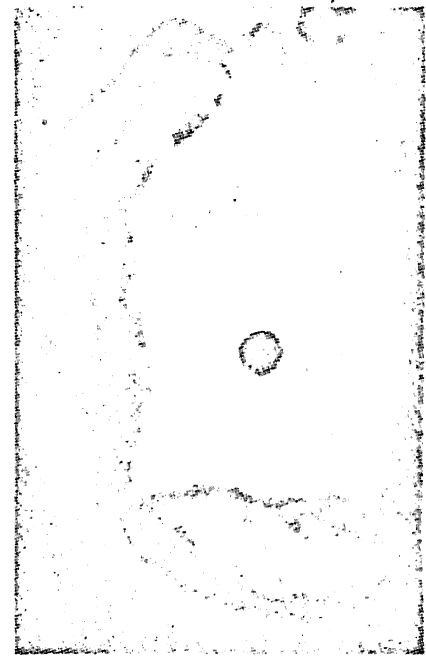


Figure 1.B  
Break-up of a toroid

extracted in the torus as a function of time of contact. The same technique can be utilized to determine the temperature profile and average temperature in a torus for heat transfer calculations.

The analytical and numerical solutions for the molecular diffusion in a cylinder are also studied to check the numerical procedures used in this work.

## II. LITERATURE REVIEW

This chapter briefly describes some of the models which are currently available for mass transfer (or heat transfer) inside droplets or bubbles. The models for both oscillating and non oscillating droplets are reviewed here. Only Kronig and Erink's model considers the effect of curvature of internal streamlines of the droplet. Handlos and Baron assumed the internal circulation pattern to be a system of tori but they have neglected the effect of torus curvature.

### Mass Transfer Mechanisms

Solute transfer between a drop and the field fluid in a spray column takes place in three stages. The first is during the period of drop formation, second is during free fall or rise of the drop and the third stage is extraction at the coalesced layer.

The mass transfer mechanisms during the formation of the droplet and the extraction at the coalescent layer are discussed elsewhere (4).

In this chapter only the mechanisms postulated for the extraction process during rise (or fall) of the droplet are discussed.

### Newman Model

Newman (8) derived a relation for mass transfer in a stagnant spherical drop using the following partial differential equation obtained from Fick's second law of diffusion.



$$\frac{\partial C_A}{\partial t} = \mathcal{D} \frac{1}{r^2} \frac{\partial}{\partial r} \left( r^2 \frac{\partial C_A}{\partial r} \right) \quad (2.1a)$$

$$C_A = C_{A_0} \quad r = r_1 \quad t = 0 \quad (2.1b)$$

$$C_A \text{ is finite} \quad r = 0 \quad t = t \quad (2.1c)$$

$$C_A = C_{A_i} \quad r = r_1 \quad t > 0 \quad (2.1d)$$

(This model assumes no continuous phase resistance, i.e.  $k_c \rightarrow \infty$ )

The solution of the above equation may be expressed as

$$E_m = 1 - \frac{6}{\pi^2} \sum_{n=1}^{\infty} \frac{1}{n^2} \exp\left(-\frac{n^2 \pi^2 \mathcal{D} t}{r_1^2}\right) \quad (2.2)$$

where  $E_m$  is the fraction of solute extracted.

The time averaged dispersed phase mass transfer coefficient may be defined as

$$k_d = -\frac{r_1}{3t} \ln(1 - E_m) \quad (2.3)$$

### Kronig and Brink Model

Kronig and Brink (7) derived a relation for droplets with internal circulation currents described by the Hadamard-Rybczinski flow patterns. These flow patterns were derived from the equations of motion simplified for the Stoke's flow regime ( $N_{Re} < 1$ ). It was assumed that the solute diffusion is only in a direction perpendicular to the internal streamlines (a condition encountered for large droplet Peclet numbers) and that continuous phase resistance is negligible. Thus the expression

for the fraction extracted is

$$E_m = 1 - \frac{3}{8} \sum_{n=1}^{\infty} B_n^2 \exp(-16\lambda_n \frac{\partial t}{r^2}) \quad (2.4)$$

and the expression for the dispersed phase mass transfer coefficient is

$$k_d = -\frac{r}{3t} \ln \left[ \frac{3}{8} \sum_{n=1}^{\infty} B_n^2 \exp(-16\lambda_n \frac{\partial t}{r^2}) \right] \quad (2.5)$$

$B_n$  and  $\lambda_n$  are given by Heertjes et al (15) for  $1 \leq n \leq 7$

### Rose and Kintner Model

Rose and Kintner (11) have developed a mass transfer model for vigorously oscillating single liquid drops moving in a liquid field which incorporates the concepts of interfacial stretch and internal droplet mixing.

To describe mass transfer from an oscillating drop, the fluid spheroid is assumed to oscillate from a nearly spherical shape to an oblate ellipsoidal shape and back to a spherical shape in one period of the oscillation. All resistance to transfer (in both continuous and dispersed phases) is assumed to be in a thin zone near the interface. The core of the drop is assumed to be well mixed. This permits a single value to represent the drop internal concentration as shown in Figure 2.1.

A material balance for the drop, based on the dispersed phase, is

$$-\frac{d(Vc_A)}{dt} = \frac{\mathcal{D}}{X} A (c_A - c_A^*) \quad (2.6)$$

where  $X$  is the thickness of the interfacial resistance zone.

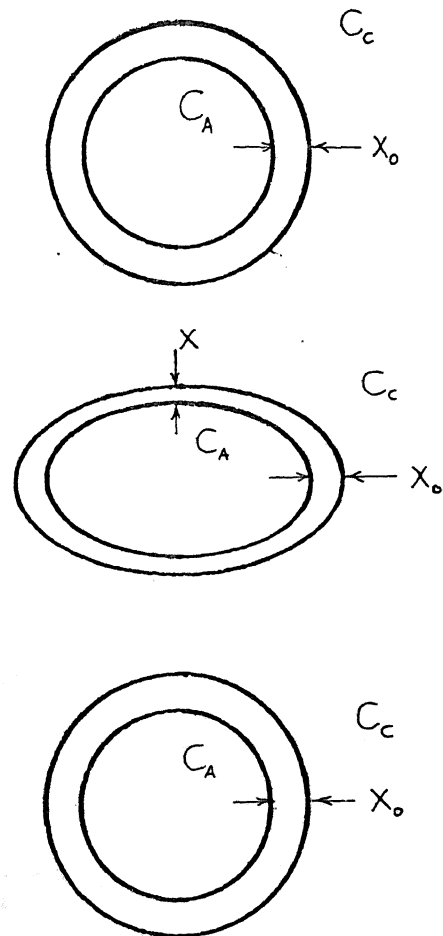


Figure 2.1 One Period of Mass Transfer Model

Since the volume of the drop is constant, the mass balance across the zone is

$$-V \frac{dc_s}{dt} = \frac{D}{X} A (C_A - C_A^*) \quad (2.7)$$

The area of an oblate ellipsoid is given by

$$A = 2\pi a^2 + \frac{\pi b^2}{\left(\frac{a^2-b^2}{a^2}\right)^{\frac{1}{2}}} \ln \left[ \frac{1 + \left(\frac{a^2-b^2}{a^2}\right)^{\frac{1}{2}}}{1 - \left(\frac{a^2-b^2}{a^2}\right)^{\frac{1}{2}}} \right] \quad (2.8)$$

By assuming that

$$a = a_0 + a_p |\sin \omega t| \quad (2.9)$$

then  $a$  varies from  $a_0$  to  $(a_0 + a_p)$ , where  $a_p$  is the amplitude of oscillation. The value of  $b$  can be found from the fact that the drop has a constant volume. Hence

$$b = \frac{3V}{4\pi a^2} \quad (2.10)$$

As the drop oscillates,  $X$  varies from  $X_0$  to  $X$  as a function of time. The value of  $X$  at any time is given by

$$X = \frac{a_0^2 b - (a - X_0)^2 (b - X_0) - 2 a b X_0 + b X_0^2}{a^2 - 2 a X_0 - X_0^2} = f_1(t) \quad (2.11)$$

To predict the initial zone thickness for spherical drop with uniform internal concentration of solute, the two film theory is used.

$$X_0 = \frac{D_E}{K_D} \quad (2.12)$$

where

$$D_E = (\text{fraction of resistance in dispersed phase}) D_D + (\text{fraction of resistance in continuous phase}) D_C \quad (2.13)$$

The frequency of oscillation,  $\omega$ , is predicted from

the equation

$$\omega^2 = \frac{\sigma b}{a^3} \frac{n(n+1)(n-1)(n+2)}{(n+1)\rho_p + n\rho_c} \quad (2.14)$$

The value of  $\omega'$  used in equation (2.9) is one half the value of  $\omega$  in equation (2.14) due to the use of the absolute value of the sine function.

Estimation of the amplitudes of drop oscillations ( $\alpha_o$  and  $\alpha_p$ ) is made from motion pictures of falling drops for the system of interest.

The solution of equation (2.6) with the boundary conditions

$$C_A = C_{A_o} \quad t = t_o \quad (2.14a)$$

$$C_A = C_{A_f} \quad t = t_f \quad (2.14b)$$

is given by

$$E = 1 - \exp \left[ -\frac{2\pi D_E}{V} \int_{t_o}^{t_f} \frac{1}{f(t)} \left\{ \left( \frac{3V}{4\pi a^2} \right)^2 \frac{1}{2\alpha} \ln \left( \frac{1+\alpha}{1-\alpha} \right) + a^2 \right\} dt \right] \quad (2.15)$$

in which

$$\alpha^2 = \frac{a^2 - \left( \frac{3V}{4\pi a^2} \right)^2}{a^2} \quad (2.16)$$

### The Surface Stretch Model

Angelo, Lightfoot and Howard (5) have developed a method for predicting rates of mass transfer through stretching or shrinking phase boundaries of finite lifetime at low mass transfer rates. They have extended the penetration theory to systems in which the area of

the mass transfer is a function of time. They limit consideration to situations in which the interface is formed suddenly at zero time between two immiscible solutions of uniform composition and to very short contact times. Diffusion in directions parallel to the interface is assumed to be negligible. With these assumptions, the continuity equation for any solute species A in either of the two phases is given by

$$\frac{\partial \rho_A}{\partial t} + v_y \frac{\partial \rho_A}{\partial y} = -\frac{\partial (j_{Ay})}{\partial y} \quad (2.17)$$

If the total mass density  $\rho$  of the solution is constant and the net rate of mass transfer is small, the fluid velocity in the neighborhood of the interface is given by

$$v_y = -y \left( \frac{\partial \ln S}{\partial t} \right)_{u,w} \quad (2.18)$$

where  $u, w$  are reference coordinates of a point in the interfacial surface and the derivative represents the local fractional rate of change (stretching) of interfacial area for a moving surface element.

For isothermal isobaric systems with no forced diffusion the mass flux is given by

$$j_{Ay} = -D_{AD} \frac{\partial \rho_A}{\partial y} \quad (2.19)$$

Equations (2.17) through (2.19) are then combined to give

$$\frac{\partial \rho_A}{\partial t} - y \left( \frac{\partial \ln S}{\partial t} \right)_{u,w} \frac{\partial \rho_A}{\partial y} = D_{AD} \frac{\partial^2 \rho_A}{\partial y^2} \quad (2.20a)$$

They have solved this equation with the aid of the boundary conditions

$$p_A = p_{A_0} \quad y > 0 \quad t = 0 \quad (2.20b)$$

$$p_A = p_{A_0} \quad y \rightarrow \infty \quad t \text{ finite} \quad (2.20c)$$

$$p_A = p_{A_0} \quad y = 0 \quad t > 0 \quad (2.20d)$$

From the solution of the above equations, the instantaneous local mass transfer coefficient may be obtained as

$$\frac{k_o}{\rho} = \left( \frac{D_{AD}}{\pi t_o} \right)^{\frac{1}{2}} \frac{S(\tau)}{\left( \int_0^{\tau} S^2(t) dt \right)^{\frac{1}{2}}} \quad (2.21)$$

where  $\tau = \frac{t}{t_o}$  and  $t_o = \frac{l}{\omega \pi}$

To compare the mass transfer behavior for variable surface area to that for the fixed area of the elementary penetration theory, they have defined a dimensionless mass transfer coefficient  $K$  in terms of reference area  $S_o$  as

$$K = \frac{k_o}{\rho} \left( \frac{D_{AD}}{\pi t_o} \right)^{\frac{1}{2}} = \frac{S(\tau)}{S_o} \left[ \int_0^{\tau} \left( \frac{S(t)}{S_o} \right)^2 dt \right]^{\frac{1}{2}} \quad (2.22)$$

The time average value of  $K$  based on the reference area  $S_o$  is defined by

$$\bar{K} = \frac{2}{\tau} \left[ \int_0^{\tau} \left( \frac{S(t)}{S_o} \right)^2 dt \right]^{\frac{1}{2}} \quad (2.23)$$

The total amount of solute  $m_A(t)$  passing through the mass transfer surface in the time interval zero to  $t$  is given by

$$m_A(t) = \bar{K} \left( \frac{D_{AD}}{\pi t_o} \right)^{\frac{1}{2}} (p_{A_0} - p_{A_\infty}) S_o t \quad (2.24)$$

As a specific case they have considered the elementary penetration theory for which  $S = S_o$ . Then from equations

(2.23) and (2.24)

$$m_A(t) = \frac{2}{(\tau)^{\frac{1}{2}}} \left( \frac{\mathcal{D}_{AD}}{\pi t_0} \right)^{\frac{1}{2}} (p_{A_0} - p_{A_\infty}) S_0 t \quad (2.25)$$

and since  $\tau = \frac{t}{t_0}$

$$m_A(t) = 2 \left( \frac{\mathcal{D}_{AD} t}{\pi} \right)^{\frac{1}{2}} (p_{A_0} - p_{A_\infty}) S_0 \quad (2.26)$$

The dimensionless mass transfer coefficient  $\bar{K}$  for several functions  $S(\tau)$  is tabulated in ( 5 ). One of these functions they have discussed is that for which

$$S(\tau) = S_0 (1 + \epsilon \sin^2 \tau) \quad (2.27)$$

with

$$t_0 = \frac{1}{\pi \omega} \quad (2.28)$$

In that case

$$\bar{K} = \frac{2}{\tau} \left[ (1 + \epsilon_0) \tau - \epsilon_1 \sin 2\tau + \epsilon_2 \sin 4\tau \right]^{\frac{1}{2}} \quad (2.29)$$

where

$$\epsilon_0 = \epsilon + \frac{3}{8} \epsilon^2 \quad (2.30a)$$

$$\epsilon_1 = \frac{\epsilon}{2} + \frac{\epsilon^2}{4} \quad (2.30b)$$

$$\epsilon_2 = \frac{\epsilon^2}{32} \quad (2.30c)$$

#### Handlos and Baron Model

Handlos and Baron (4) have proposed a dispersed phase transfer mechanism which shows promise in predicting the very low resistance to mass transfer inside circulating and/or oscillating droplets. Their eddy diffusion model is devoid of any constant or parameter which must be obtained from experimental measurements. However, it is assumed that the velocities of continuous and dispersed



phase are known and the velocity of falling (or rising) droplets can be predicted (15).

The model is based on the assumption that internal circulation is fully developed. The circulation pattern within the spherical droplet is assumed to be a system of tori. The cross sectional view of the drop is given in Figure 2.2. Handlos and Baron further assumed that "random radial vibrations" are superimposed upon the streamlines. Handlos and Baron do not specifically state the source of these vibrations, but oscillation of the droplets is one likely source. Turbulence due to circulation is another possible source. The mixing between streamlines is due to these vibrations which are the key to their eddy diffusion mechanism. The entire transfer process is assumed to take place within the outer surface of the torus.

The differential mass balance on the system within the torus is (15)

$$\frac{\partial c_A}{\partial t} = \nabla \cdot (\bar{E} \nabla c_A) \quad (2.31)$$

They assumed that the Einstein diffusion equation for two dimension applies.

$$\bar{E} = \frac{Z^2}{4t} \quad (2.32)$$

where  $Z^2$  is the mean square displacement of an element of fluid during the average circulation time of the element, and it is given by

$$Z^2 = \frac{d^2}{96} (6r^2 - 8r - 3) \quad (2.33)$$

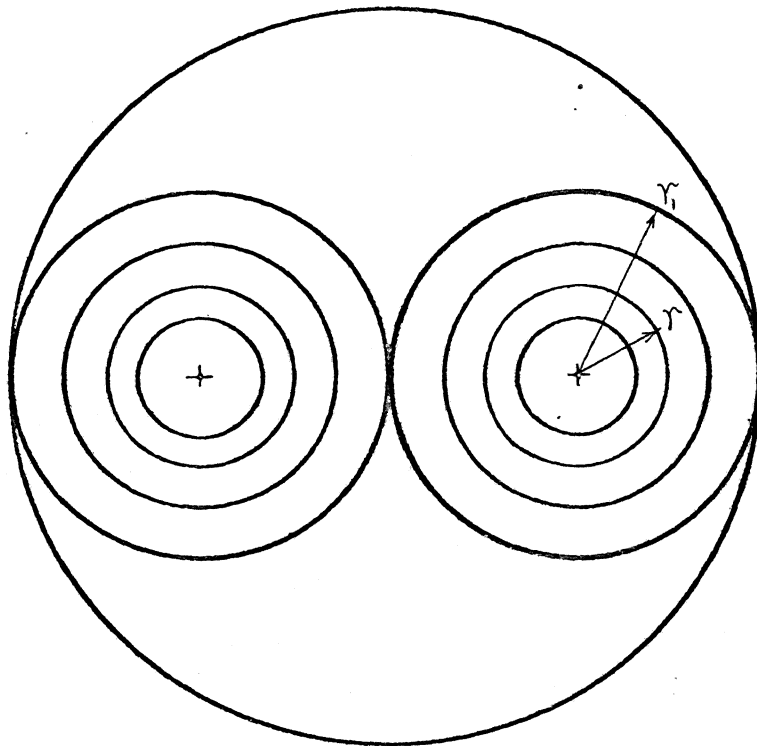


Figure 2.2 Handlos & Baron Stream Lines

Handlos and Baron further assumed that  $\bar{t}$  for their model can be approximated by the value of  $\bar{t}$  for Hadamard-Rybezinski internal circulation velocities and pattern for laminar circulation.

Thus

$$\bar{t} \approx \frac{16}{3} \frac{d}{u} \left(1 + \frac{u_d}{u_c}\right) \quad (2.34)$$

Substitution of equations (2.33) and (2.34) in (2.32) gives the relation for eddy diffusivity

$$\bar{E} = \frac{u(6r^2 - 8r + 3)d}{2048 \left(1 + \frac{u_d}{u_c}\right)} \quad (2.35)$$

Handlos and Baron derived their model in cylindrical co-ordinates assuming an infinite cylinder for the system of tori. Therefore, equation (2.31) becomes

$$\frac{\partial c_a}{\partial t} = \frac{1}{r} \frac{\partial}{\partial r} \left( \bar{E} \frac{\partial c_a}{\partial r} \right) \quad (2.36)$$

Thus they assumed, the mass transfer is only in radial direction and the effect of the torus curvature is negligible. Then equations (2.31) through (2.35) are combined to give

$$\frac{\partial c_a}{\partial t} = \frac{b}{1-y} \frac{\partial}{\partial y} \left[ (1 - 5y + 10y^2 - 6y^3) \frac{\partial c_a}{\partial y} \right] \quad (2.37)$$

where

$$b = \frac{u}{128 \left(1 + \frac{u_d}{u_c}\right) d} \quad (2.38)$$

and

$$r = 1 - y \quad (2.39)$$

They employed the following boundary conditions :

$$C_A = 0 \quad y = 0 \quad t > 0 \quad (2.40a)$$

$$C_A \quad y = 1 \quad t = t \quad (2.40b)$$

$$C_A = C_{A_0} \quad 0 < y < 1 \quad t = 0 \quad (2.40c)$$

Thus with equation (2.37) and the boundary conditions, the following expression is obtained.

$$E_m = 1 - 2 \sum_{n=1}^N B_n^2 \exp(-\lambda_n^2 bt) \quad (2.41)$$

where four values of  $\lambda_n$  are available (15).

The dispersed phase mass transfer coefficient is defined as

$$k_d = -\frac{d}{6t} \ln(1 - E_m) \quad (2.42)$$

For large contact times, only the first term of the series solution is dominant. Therefore, by considering just the first term in a series solution, equations (2.41) and (2.42) lead to the following formulation of the mass transfer coefficient:

$$k_d = \frac{\lambda_1 u}{768(1 + \frac{u}{u_c})} \quad (2.43)$$

Handlos and Baron considered the case of zero continuous phase resistance and found  $\lambda_1 = 2.88$ .

It can be seen that Handlos and Baron have neglected the effect of torus curvature. In the following chapter, mathematical model for molecular diffusion to a torus is derived. This will give some insight into the effect of torus curvature on diffusion.

### III. MATHEMATICAL MODEL

#### Diffusion Equation For A Torus Body

The equation of continuity in mass units is given by (1).

$$\frac{\partial \rho_A}{\partial t} + \nabla \cdot \bar{n}_A = r_A \quad (3.1)$$

where

$$\bar{n}_A = w_A \bar{n} - \rho \mathcal{D}_{AB} \nabla W_A \quad (3.2)$$

$$w_A = \frac{\rho_A}{\rho} \quad (3.3)$$

$$\bar{n} = \rho \bar{v} \quad (3.4)$$

Therefore,

$$w_A \bar{n} = \frac{\rho_A}{\rho} (\rho \bar{v}) = \rho_A \bar{v} \quad (3.5)$$

From equations (3.2) and (3.5)

$$\bar{n}_A = \rho_A \bar{v} - \rho \mathcal{D}_{AB} \nabla W_A \quad (3.6)$$

Hence, equation (3.1) reduces to

$$\frac{\partial \rho_A}{\partial t} - (\nabla \cdot \rho_A \bar{v}) = \nabla \cdot \rho \mathcal{D}_{AB} \nabla W_A + r_A \quad (3.7)$$

If constant density and diffusivity are assumed, equation (3.7) becomes

$$\frac{\partial \rho_A}{\partial t} + \rho_A (\nabla \cdot \bar{v}) + (\bar{v} \cdot \nabla \rho_A) = \mathcal{D}_{AB} \nabla^2 \rho_A + r_A \quad (3.8)$$

For a fluid of constant density  $\nabla \cdot \bar{v}$  is zero.

Dividing equation (3.8) by molecular weight, one obtains

$$\frac{\partial C_A}{\partial t} + (\bar{v} \cdot \nabla C_A) = \mathcal{D}_{AB} \nabla^2 C_A + R_A \quad (3.9)$$

If there are no chemical changes and  $\bar{v}$  is zero (or very small), then equation (3.9) reduces to

$$\frac{\partial C_A}{\partial t} = \mathcal{D}_{AB} \nabla^2 C_A \quad (3.10)$$

This is known as Fick's second law of molecular diffusion.

The parametric equations for a torus (13) are

$$x = (a + r \sin \theta) \cos \phi \quad (3.11)$$

$$y = (a + r \sin \theta) \sin \phi \quad (3.12)$$

$$z = r \cos \theta \quad (3.13)$$

The part of the surface of the torus in the first octant is shown in Figure 3.1. Fick's second law in orthogonal-toroidal coordinates is (refer to appendix A)

$$\frac{\partial C_A}{\partial t} = \frac{D_{AB}}{r(a+r\sin\theta)} \left\{ \frac{\partial}{\partial r} \left[ r(a+r\sin\theta) \frac{\partial C_A}{\partial r} \right] + \frac{\partial}{\partial \theta} \left[ \frac{a+r\sin\theta}{r} \frac{\partial C_A}{\partial \theta} \right] + \frac{\partial}{\partial \phi} \left[ \frac{r}{(a+r\sin\theta)} \frac{\partial C_A}{\partial \phi} \right] \right\} \quad (3.14)$$

Due to the symmetry of the torus,  $\frac{\partial C_A}{\partial \phi}$  equals to zero. Thus the partial differential equation for diffusion to a torus is

$$\frac{1}{D_{AB}} \frac{\partial C_A}{\partial t} = \frac{\partial^2 C_A}{\partial r^2} + \frac{1}{r} \frac{\partial C_A}{\partial r} + \frac{\sin \theta}{(a+r\sin\theta)} \frac{\partial C_A}{\partial r} + \frac{1}{r^2} \frac{\partial^2 C_A}{\partial \theta^2} + \frac{\cos \theta}{r(a+r\sin\theta)} \frac{\partial C_A}{\partial \theta} \quad (3.15a)$$

The boundary conditions are

$$C_A = C_{A_0} \quad t = 0 \quad 0 \leq r < r_1 \quad 0 \leq \theta \leq 2\pi \quad (3.15b)$$

$$C_A = C_{A_1} \quad t > 0 \quad r = r_1 \quad 0 \leq \theta \leq 2\pi \quad (3.15c)$$

$$\frac{\partial C_A}{\partial \theta} = 0 \quad t > 0 \quad 0 \leq r < r_1 \quad \theta = \frac{\pi}{2}, \frac{3\pi}{2} \quad (3.15d)$$

In terms of the dimensionless variables

$$R = \frac{r}{r_1} \quad (3.16)$$

$$A = \frac{a}{r_1} \quad (3.17)$$

$$\tau = \frac{D_{AB} t}{r_1^2} \quad (3.18)$$

$$C = \frac{C_A - C_{A_1}}{C_{A_0} - C_{A_1}} \quad (3.19)$$

equation (3.15a) transforms into

$$\frac{\partial C}{\partial \tau} = \frac{\partial^2 C}{\partial R^2} + \left( \frac{1}{R} + \frac{\sin \theta}{A + R \sin \theta} \right) \frac{\partial C}{\partial R} + \frac{1}{R^2} \frac{\partial^2 C}{\partial \theta^2} + \frac{\cos \theta}{R(A + R \sin \theta)} \frac{\partial C}{\partial \theta} \quad (3.20a)$$

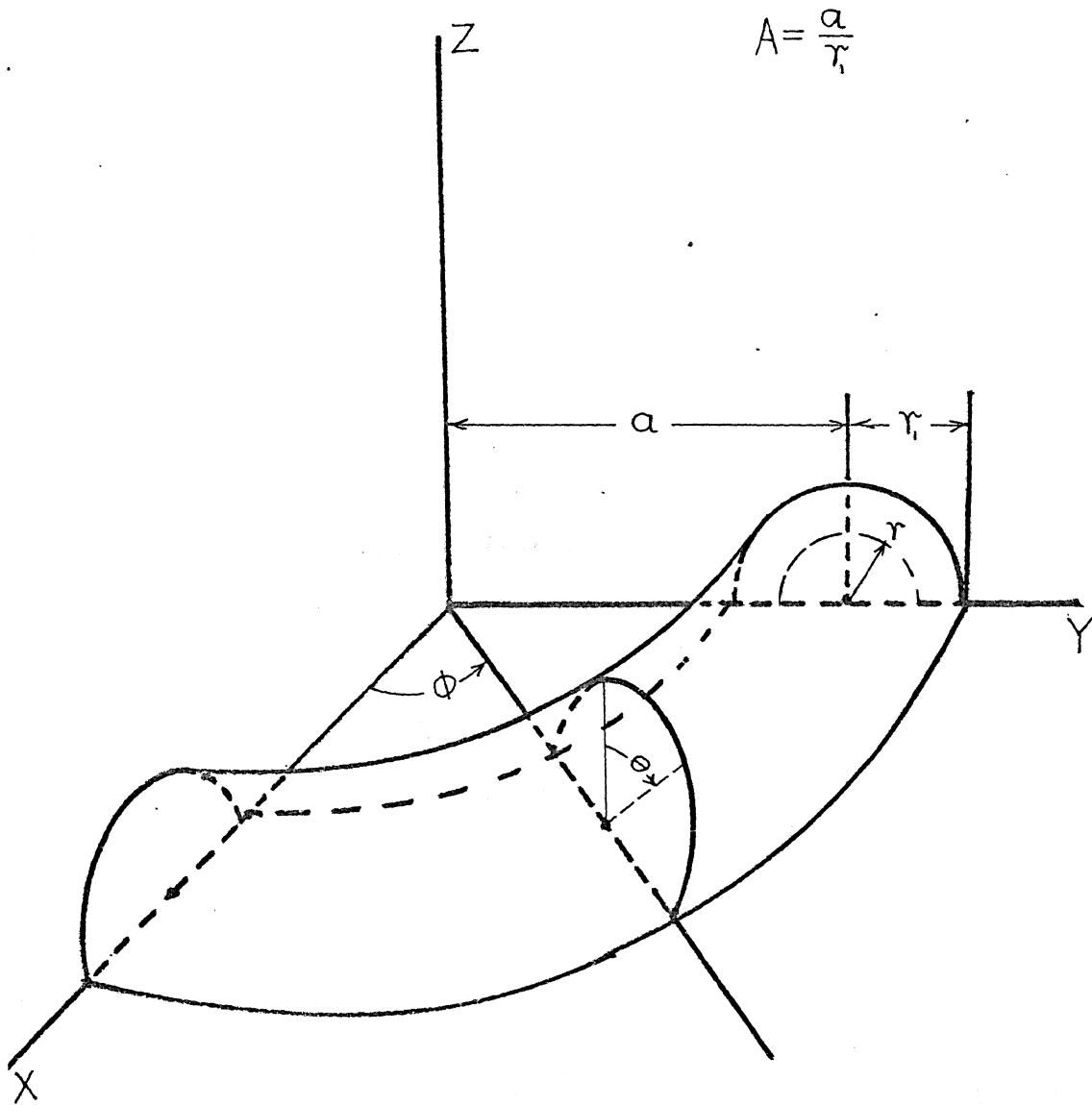


Figure 3.1 A Part of the Torus

and the boundary conditions become

$$C = 1 \quad \gamma = 0 \quad 0 \leq R < 1 \quad 0 \leq \theta \leq 2\pi \quad (3.20b)$$

$$C = 0 \quad \gamma > 0 \quad R = 1 \quad 0 \leq \theta \leq 2\pi \quad (3.20c)$$

$$\frac{\partial C}{\partial \theta} = 0 \quad \gamma > 0 \quad 0 \leq R < 1 \quad \theta = \frac{\pi}{2}, \frac{3\pi}{2} \quad (3.20d)$$

For  $A = \infty$ , the terms containing  $A$  in equation (3.20a)

equal to zero and it becomes

$$\frac{\partial C}{\partial \gamma} = \frac{\partial^2 C}{\partial R^2} + \frac{1}{R} \frac{\partial C}{\partial R} + \frac{1}{R^2} \frac{\partial^2 C}{\partial \theta^2} \quad (3.20e)$$

Equation (3.20e) describes diffusion to an infinite cylinder.

#### A Coordinate Transformation:

The numerical solution of equation (3.20a) in the rectangular  $\gamma, \theta$  plane introduces some awkward problems. In particular the point  $\gamma=0$  in the  $\gamma, \theta$  plane becomes the line  $\gamma=0$  in the rectangular  $\gamma, \theta$  plane and the only boundary condition available along this line is the condition that  $C(0, \theta, \gamma)$  is finite and independent of  $\theta$ .

As a result, a transformation from the orthogonal-toroidal co-ordinate system to cylindrical  $x, z, \phi$  coordinate system is introduced and the solution to equation (3.20a) is carried out in the rectangular  $x, z$  plane. The transformation is given by

$$X = \frac{x-a}{r_i} = \frac{r}{r_i} \sin \theta = R \sin \theta \quad (3.21)$$

$$Z = \frac{z}{r_i} = \frac{r}{r_i} \cos \theta = R \cos \theta \quad (3.22)$$

and equation (3.20a) becomes

$$\frac{\partial C}{\partial \gamma} = \frac{\partial^2 C}{\partial X^2} + \frac{1}{A+X} \frac{\partial C}{\partial X} + \frac{\partial^2 C}{\partial Z^2} \quad (3.23a)$$



The boundary conditions transform into

$$C(X, Z, 0) = 1 \quad (3.23b)$$

$$C(X, \pm\sqrt{1-X^2}, \tau) = 0 \quad (3.23c)$$

$$\frac{\partial C}{\partial Z}(X, 0, \tau) = 0 \quad (3.23d)$$

where  $-1 \leq X \leq 1$ ,  $0 \leq Z \leq 1$ ,  $X^2 + Z^2 \leq 1$

#### IV. THE SOLUTION

In this chapter, the formulas for the concentration profile, the volumetric average concentration and the fraction extracted as a function of time are derived.

##### The Method of Solution

The solution of equation (3.23a) with its boundary conditions is difficult to obtain by the usual procedures of mathematical physics, as a result, a numerical technique has been employed.

The numerical method selected to solve the model is the finite difference technique (3, 6, 9, 12). The explicit finite difference method is chosen over the implicit finite difference method for the following reasons: (1) The explicit method gives sufficiently accurate results; (2) It is easier to program on a computer; and (3) For partial differential equations with three independent variables, the explicit methods have been partially developed in the literature (12). The most important advantage of the implicit methods over the explicit methods is that for a given accuracy the implicit methods are faster.

The difference equations which approximate equation (3.23a) are defined at a finite set of points as shown in Figure 4.1.

In a torus, symmetry is assumed about the angle  $\phi$  and the line  $Z=0$  or  $\theta=\frac{\pi}{2}$  and  $\frac{3\pi}{2}$ . Therefore the point concentration profile is required only for a semicircle

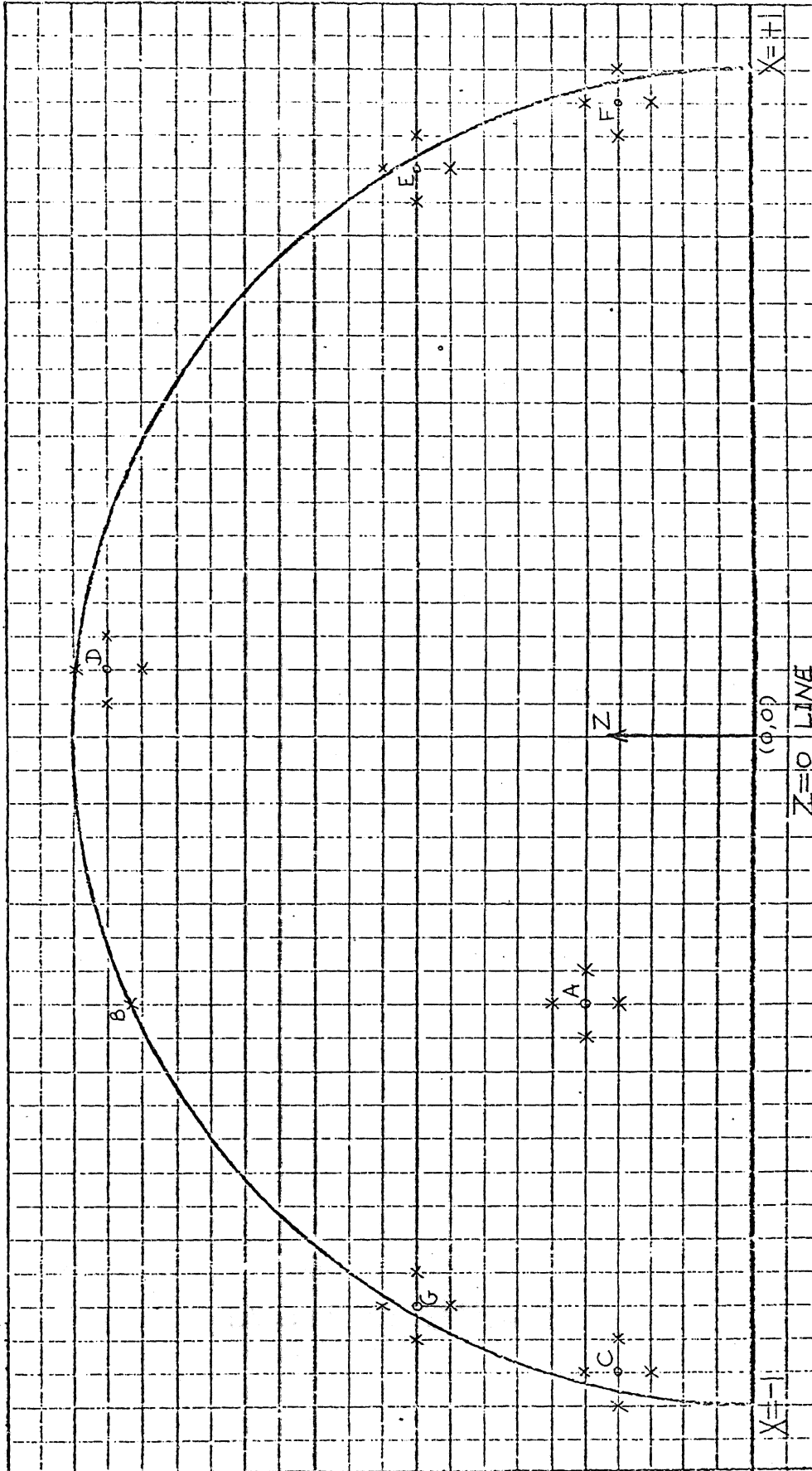


Figure 4.1 Net Work

set of points.

There are five different types of nodal points which have to be considered in the calculations. These are as follows: (1) The points which have each adjoining point spaced a complete increment  $\Delta X$  from it, (for example, point A in Figure 4.1); (2) The points located along the line  $Z=0$ ; (3) The points near the boundary, (for example, nodal points C, F and D in Figure 4.1); (4) The points near the boundary in which two of their neighboring nodes are between them and the boundary, (for example, nodal points E and G in Figure 4.1); (5) The points on the boundary, (for example, point B). The points of these five types are denoted as the sets ES, SP, UE1, UE2 and BP, respectively.

#### Classical Explicit Method:

The partial derivatives of equation (3.23a) are approximated by the following finite differences:

$$\frac{\partial C}{\partial \tau} = \frac{C_{i,j,k+1} - C_{i,j,k}}{\Delta \tau} \quad (4.1)$$

$$\frac{\partial C}{\partial X} = \frac{C_{i+1,j,k} - C_{i-1,j,k}}{2 \Delta X} \quad (4.2)$$

$$\frac{\partial^2 C}{\partial X^2} = \frac{C_{i+1,j,k} - 2C_{i,j,k} + C_{i-1,j,k}}{(\Delta X)^2} \quad (4.3)$$

$$\frac{\partial^2 C}{\partial Z^2} = \frac{C_{i,j+1,k} - 2C_{i,j,k} + C_{i,j-1,k}}{(\Delta Z)^2} \quad (4.4)$$

Equation (3.23a) then becomes

$$\begin{aligned} \frac{C_{i,j,k+1} - C_{i,j,k}}{\Delta \tau} = & \frac{C_{i+1,j,k} - 2C_{i,j,k} + C_{i-1,j,k}}{(\Delta X)^2} + \frac{1}{A+X} \frac{C_{i+1,j,k} - C_{i-1,j,k}}{2 \Delta X} \\ & + \frac{C_{i,j+1,k} - 2C_{i,j,k} + C_{i,j-1,k}}{(\Delta Z)^2} \end{aligned} \quad (4.5)$$

Setting  $\Delta X = \Delta Z$  and  $S = \frac{\Delta \tau}{(\Delta X)^2}$ , and rearranging equation (4.5), one obtains

$$C_{i,j,k+1} = \left(S + \frac{1}{A+X} \frac{S \cdot \Delta X}{2}\right) C_{i+1,j,k} + \left(S + \frac{1}{A+X} \frac{S \cdot \Delta X}{2}\right) C_{i-1,j,k} \\ + (S) C_{i,j+1,k} - (S) C_{i,j-1,k} + (1 - 4S) C_{i,j,k} \quad (4.6)$$

where  $i$  corresponds to the  $x$  axis

$j$  corresponds to the  $z$  axis

Thus  $C_{i,j,k}$  is the concentration at the nodal point  $(I, J)$  on " $\tau = k$ " plane.

#### Finite Difference Equations

The overall scheme of solution is to calculate the concentration profile for each spatial plane  $(X, Z)$  from the values of the previous plane. This is illustrated in Figure 4.2. From the boundary conditions of equation (3.23a), the concentration profile in the plane  $\tau = 0$  is known. The concentrations at the points in sets ES, SP, UE1 and UE2 are unity and the concentrations at the points in the set BP are zero. The concentrations in the plane  $\tau = \Delta \tau$  are calculated by the explicit method from the points in the  $\tau = 0$  plane (point CE in Figure 4.2). This procedure is then repeated for the next time step.

The finite difference equations for different sets are derived as follows:

(1) For ES set. Equation (4.6) applies for calculation of concentrations at points in the ES set.

(2) For SP set. Equation (4.6) for the points on  $z = 0$  line takes the following form

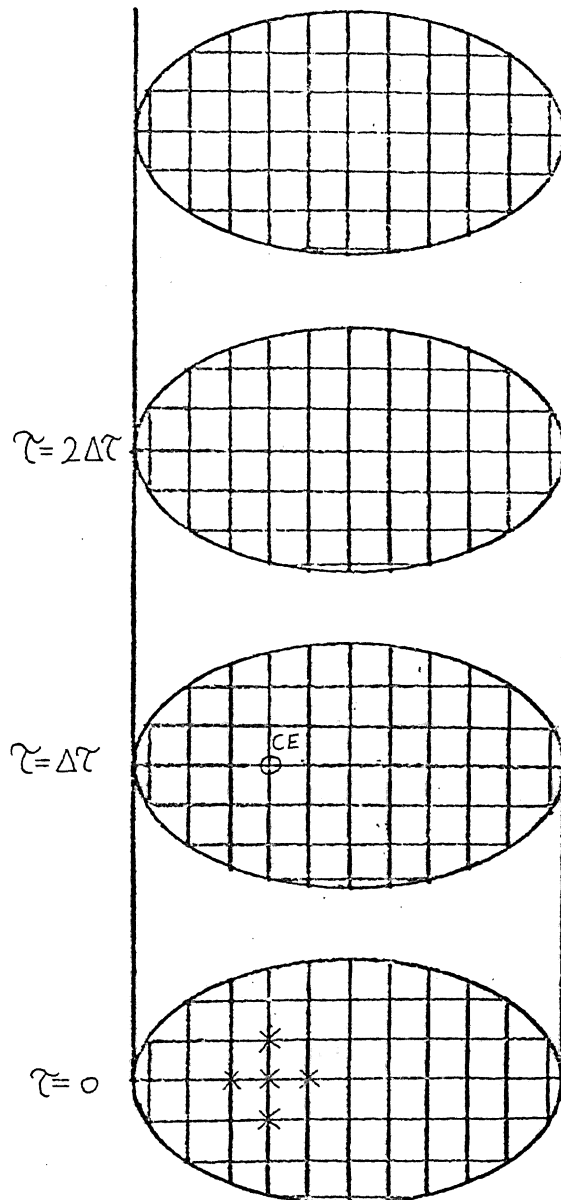


Figure 4.2 Three Dimensional Explicit Method Pattern

$$C_{i,0,k} = \left( S + \frac{1}{A+X} \frac{S \cdot \Delta X}{2} \right) C_{i+1,0,k} + \left( S - \frac{1}{A+X} \frac{S \cdot \Delta X}{2} \right) C_{i-1,0,k} \\ + (S) C_{i,1,k} + (S) C_{i,-1,k} + (1-4S) C_{i,0,k} \quad (4.7)$$

From the symmetry condition (3.23d)

$$C_{i,-1,k} = C_{i,1,k} \quad (4.8)$$

Therefore,

$$C_{i,0,k} = \left( S + \frac{1}{A+X} \frac{S \cdot \Delta X}{2} \right) C_{i+1,0,k} + \left( S - \frac{1}{A+X} \frac{S \cdot \Delta X}{2} \right) C_{i-1,0,k} \\ + (2S) C_{i,1,k} + (1-4S) C_{i,0,k} \quad (4.9)$$

(3) For sets UE1 and UE2. The concentrations at the nodes located at unequal increments near the boundary are calculated by means of a linear interpolation formula since the normal five point formula is not applicable.

Thus equation (4.6) is modified by the following procedure:

The linear interpolation formulas for the points of the sets UE1 and UE2 are

$$\frac{C_B - C_{i \pm 1, j, k+1}}{C_{i, j, k+1} - C_{i \pm 1, j, k+1}} = \frac{ALX \cdot \Delta X}{\Delta X} \quad (4.10)$$

and

$$\frac{C_B - C_{i, j-1, k+1}}{C_{i, j, k+1} - C_{i, j-1, k+1}} = \frac{ALZ \cdot \Delta Z}{\Delta Z} \quad (4.11)$$

where  $\Delta X = \Delta Z$

$(ALX)\Delta X$  and  $(ALZ)\Delta X$  are the distances of the points  $C_{i \pm 1, j, k+1}$  and  $C_{i, j-1, k}$  from the boundary, respectively; and  $C_B$  is the concentration of the point on the boundary. The above equations [(4.10) and (4.11)] are used, depending upon the close neighborhood of these points from the boundary,

either in the X or Z direction.

For negative values of X, equation (4.10) becomes

$$\frac{C_B - C_{i+1,j,k+1}}{C_{i,j,k+1} - C_{i+1,j,k+1}} = \frac{ALX \cdot \Delta X}{\Delta X} \quad (4.12)$$

Let  $C_B$  be denoted as BC. Rearranging equation (4.12), one obtains

$$C_{i,j,k+1} = \frac{BC - (TH)C_{i+1,j,k+1}}{ALX} \quad (4.13)$$

where  $TH = 1 - ALX$

The equation for  $C_{i+1,j,k+1}$  can be obtained from (4.6) on replacing  $i$  by  $i+1$ .

Therefore, equation (4.13) becomes

$$C_{i,j,k+1} = BC - TH \left[ \left( S + \frac{1}{A+X} \frac{S \cdot \Delta X}{2} \right) C_{i+2,j,k} + \left( S - \frac{1}{A+X} \frac{S \cdot \Delta X}{2} \right) C_{i,j,k} + \right. \\ \left. (S)C_{i+1,j+1,k} + (S)C_{i+1,j-1,k} + (1-4S)C_{i+1,j,k} \right] / ALX \quad (4.14)$$

Similarly for positive values of X

$$C_{i,j,k+1} = \frac{BC - (TH)C_{i-1,j,k+1}}{ALX} \quad (4.15)$$

The equation for  $C_{i-1,j,k+1}$  can be obtained from equation (4.6) on replacing  $i$  by  $i-1$ .

Therefore, equation (4.15) becomes

$$C_{i,j,k+1} = BC - TH \left[ \left( S + \frac{1}{A+X} \frac{S \cdot \Delta X}{2} \right) C_{i,j,k} + \left( S - \frac{1}{A+X} \frac{S \cdot \Delta X}{2} \right) C_{i-2,j,k} + \right. \\ \left. (S)C_{i-1,j+1,k} + (S)C_{i-1,j-1,k} + (1-4S)C_{i-1,j,k} \right] / ALX \quad (4.16)$$



When  $ALZ$  is less than  $ALX$ , the linear interpolation formula (4.11) is used for both negative and positive values of  $X$ .

On rearranging equation (4.11)

$$C_{i,j,k+1} = \frac{BC - (TH)C_{i,j-1,k+1}}{ALZ} \quad (4.17)$$

The equation for  $C_{i,j-1,k+1}$  can be obtained from equation (4.6) on replacing  $j$  by  $j-1$ .

Therefore, equation (4.17) becomes

$$C_{i,j,k+1} = BC - TH \left[ \left( S + \frac{1}{A+X} \frac{S \cdot \Delta X}{2} \right) C_{i+1,j-1,k} + \left( S - \frac{1}{A+X} \frac{S \cdot \Delta X}{2} \right) C_{i-1,j-1,k} + (S)C_{i,j,k} + (S)C_{i,j-2,k} + (1-4S)C_{i,j-1,k} \right] / ALZ \quad (4.18)$$

#### Volumetric Average Concentration

After obtaining the point concentrations from the numerical solution of equation (3.23a), the volumetric average concentration is determined as follows: (6).

By definition

$$\bar{C}(\tau) = \frac{\int_V C(x,z,\tau) dv}{\int_V dv} \quad (4.19)$$

The elemental volume  $dv$  of the torus for the numerical calculations is given by the following equation

$$dv = 2\pi(A+X)dx \cdot dz \quad (4.20)$$

so that

$$\bar{C}(\tau) = \frac{4\pi \int_{-1}^1 (A+X) dx \int_0^{\sqrt{1-x^2}} C(x,z,\tau) dz}{2\pi^2 A} \quad (4.21)$$

The volumetric average concentration is then determined by numerical integration of equation (4.21) as shown in appendix B. The fraction extracted is calculated from the following equation:

$$E_m = 1 - \bar{C}(\tau) \quad (4.22)$$

#### Analytical Solution For A Cylinder

For molecular diffusion into a cylinder, the equations for calculation of the point and average concentrations are discussed in appendix C.

As mentioned earlier in this work, the solutions for the torus will be compared with that for an infinite cylinder.

#### Computational Error

Let  $C$  denote the exact solution of the difference equation and  $C$  the exact solution of the differential equation, both solutions satisfying the given boundary and initial conditions. If  $C$  is substituted into the difference equation (4.6), there will be a remainder term or truncation error, so that

$$\begin{aligned} C_{i,j,k+1} = & \left( S - \frac{1}{A+X} \frac{S \cdot \Delta X}{2} \right) C_{i+1,j,k} + \left( S - \frac{1}{A+X} \frac{S \cdot \Delta X}{2} \right) C_{i-1,j,k} \\ & + (S) C_{i,j+1,k} + (S) C_{i,j-1,k} + (1 - 4S) C_{i,j,k} + T_{ij} \end{aligned} \quad (4.23)$$

where  $T_{ij}$  is the truncation error.

Assuming that  $C$  has continuous partial derivatives with respect to  $X$  and  $Z$  of order four, truncation error equation derived in appendix D is

$$\tau_{ij} = \frac{1}{2} \Delta\tau \frac{\partial^2 c}{\partial \tau^2} - \frac{1}{6(A+X)} (\Delta X)^2 \frac{\partial^3 c}{\partial X^3} - \frac{1}{12} (\Delta X)^2 \left( \frac{\partial^4 c}{\partial X^4} + \frac{\partial^4 c}{\partial Z^4} \right) \quad (D.10)$$

$$\text{and} \quad \tau_{ij} = O(\Delta\tau) + O(\Delta X)^2 \quad (D.11)$$

Thus, the truncation error is a function of  $A$  and step sizes. In order to reduce the magnitude of the truncation error, both  $\Delta\tau$  and  $\Delta X$  should be very small. It can be seen from (D.11) that if mesh size and the time step are increased in the same proportion, the error introduced by the change in the time step will be more than that for the change in the mesh size.

### Stability

In addition to convergence of the finite difference equation, stability is essential in the sense that inevitable rounding errors in the calculation must not swamp the true finite difference solution.

The stability criteria for parabolic partial differential equations with constant coefficient and two or three independent variables are discussed in the references (3, 9, 11). The stability criterion for the finite difference equation approximation of the parabolic equation of the type

$$\frac{\partial c}{\partial \tau} = \frac{\partial^2 c}{\partial X^2} + \frac{\partial^2 c}{\partial Z^2}$$

$$\text{is } \frac{\Delta\tau}{(\Delta X)^2} \leq \frac{1}{4} \quad (\text{for a square mesh}) \quad (8).$$

Equation (3.23a) consists of an additional lower order partial derivative with a variable coefficient.

It is reported (3) that the presence of the lower order

term in differential equation has no great effect on the stability criterion, in comparison to higher order terms, in the formation of difference equation. Therefore the stability criterion for the finite difference equation of equation (3.23a) can be expected to be similar to the above equation.

Values of  $\frac{\Delta \tau}{(\Delta x)^2}$  greater than 0.25 were tried as a test but the solutions were found to be unstable.

## V. RESULTS AND DISCUSSION

### Point Concentrations

As described in the previous chapter, the point concentrations were calculated as a function of time for various values of the parameter  $A$ . The parameter  $A$  appearing in the partial differential equation (3.20a) has a definite physical significance. The two extreme values of  $A$  transform this equation to the diffusion equations for a stagnant sphere and a cylinder. When  $A=0$  in equation (3.20a), it describes molecular diffusion into a sphere; and for  $A \rightarrow \infty$ , it reduces to the case of diffusion in an infinite cylinder. Since a torus is a solid of revolution obtained by rotating a circle of radius  $r$  at a distance  $a$  from the  $x$ -axis, the sphere is a special case when  $a=0$ .

Thus there is a certain similarity in the molecular diffusion equations for a torus, a sphere and a cylinder. However, the parameter  $A$  in the diffusion equation for a torus is attributed to the dissymmetry of the concentration profile. For molecular diffusion into a sphere or cylinder, the concentration profile is symmetrical about both the coordinate axes.

The concentrations for different values of  $A$  at  $x = \pm 0.8$  ( $Z=0$  line) are shown in Tables (5.1, 5.2 and 5.3) to illustrate the dissymmetry of the concentration profile. The variation of the point concentration with time is presented in Figures 5.2 and 5.3.

It can be observed that the concentration at  $X = -0.8$  is higher than at  $X = +0.8$ . This could be explained as follows.

Referring to Figure 5.4, the points  $X = +0.8$  and  $X = -0.8$  are in the semicircles ABD and ACD, respectively. The surface of the revolution obtained by revolving the arc ABD about the Z axis is larger than the surface of the revolution generated by the arc ACD. Since the torus surface comprises of these two surfaces, the surface area of the right half of the torus is larger than the left half. The magnitudes of these areas are  $2\pi^2 a r_1 (1 + \frac{2}{\pi})$  and  $2\pi^2 a r_1 (1 - \frac{2}{\pi})$  respectively, and their ratio is  $(1 + \frac{2}{\pi}) / (1 - \frac{2}{\pi})$ . Thus the total transport of the solute on the torus surface should be more near  $X = +0.8$  than near  $X = -0.8$ . Consequently the concentration is less at  $X = +0.8$  than the value of the concentration at  $X = -0.8$ . This is true for all the points in the right-half portion of the torus.

For large values of A, the difference in the values of the concentrations at these points is smaller (refer to Table 5.8). The value of A determines the curvature of the torus. When A is small, the effect of the torus curvature is predominant and hence the difference in the concentrations at  $X = \pm 0.8$  (diametrically opposite points) is large. As A increases, this difference diminishes and for  $A \rightarrow \infty$ , concentrations are equal. Thus for large values of A, the concentration profile tends to be symmetrical. When the value of A is very large the

solution should approach that for an infinite cylinder (in which case, the concentration profile is symmetrical).

The values of the concentration at the center of the torus are shown in Table (5.10). As  $A$  increases, the concentration decreases because of the corresponding increase in the surface area.

#### Fraction Extracted

The dimensionless average concentration is calculated as shown in appendix B. The fraction extracted for various values of dimensionless time and  $A$  is given in Tables (5.1, 5.2 and 5.3). The fraction extracted is approximately the same for all values of  $A$ ; this might be expected since the surface area to volume ratio ( $2/\gamma$ ) is independent of  $A$ . Geometrically the torus is a bent cylinder, and hence the fraction extracted from torus is nearly the same as for a cylinder. Therefore a single graph is plotted for the fraction extracted versus the dimensionless time regardless of the value of  $A$ .

The values of the fraction extracted for a torus and cylinder are not exactly the same, possibly because of the computational error. The truncation error formula is derived in appendix D. It is a function of  $A$ . The results for a cylinder and a torus show that the value of the point concentration at diametrically opposite points in a cylinder is between the values of concentrations at these points in a torus. Thus the parameter  $A$  introduces dissymmetry in the concentration

profile but does not change the value of the fraction extracted.

#### Effect of Mesh Size on Numerical Solution

The mesh size  $\Delta X=0.05$  was changed to 0.04. The time step had to be changed to  $\Delta \tau=0.0003$  to satisfy the stability criterion. The results obtained are given in Tables (5.5, 5.6 and 5.7). As expected, the smaller mesh size gives slightly more accurate results, but the difference in the results obtained due to a change in the mesh size is insignificant at large contact times.

#### Analytical Solution for a Cylinder

The point concentration and fraction extracted for diffusion from a cylinder were obtained from the equations discussed in appendix C. These analytical solutions were derived for diffusion in the radial direction only.

The point concentration at  $R=0.8$  and fraction extracted are given in Table (5.4). These results are compared with the numerical solution obtained for a cylinder in which diffusion in  $\Theta$  direction is also considered. However, because of symmetry in  $\Theta$  direction both the results are nearly identical.



TABLE(5.1)

DISSYMMETRY OF THE CONCENTRATION PROFILE  
( $\Delta = 1$ ,  $\Delta\tau = 0.0005$ ,  $\Delta X = 0.05$ )

Dimensionless time (TAU)	Dimensionless Concentration (C)		Fraction Extracted (Em)
	X = -0.8	X = +0.8	
0.002	0.99956	0.99881	0.11234
0.004	0.97899	0.95449	0.14928
0.006	0.95216	0.89707	0.17763
0.008	0.92627	0.84197	0.20145
0.01	0.90257	0.79224	0.22233
0.012	0.88104	0.74798	0.24109
0.014	0.86146	0.70864	0.25823
0.016	0.84356	0.67354	0.27408
0.018	0.82709	0.64205	0.28887
0.02	0.81186	0.61366	0.30276
0.04	0.70104	0.43063	0.41110
0.06	0.62771	0.33358	0.48912
0.08	0.57097	0.27125	0.55111
0.10	0.52325	0.22690	0.60270
0.11	0.50156	0.20903	0.62555
0.12	0.48093	0.19328	0.64676
0.13	0.46117	0.17926	0.66654
0.14	0.44214	0.16668	0.68502
0.15	0.42375	0.15531	0.70233
0.16	0.40594	0.14499	0.71358
0.17	0.38868	0.13557	0.73385
0.18	0.37195	0.12694	0.74823
0.19	0.35572	0.11900	0.76177
0.20	0.34001	0.11167	0.77454
0.21	0.32480	0.10490	0.78659
0.22	0.31009	0.09861	0.79796
0.23	0.29590	0.09277	0.80870
0.24	0.28221	0.08734	0.81886
0.25	0.26902	0.08227	0.82845
0.26	0.25634	0.07754	0.83753
0.27	0.24415	0.07311	0.84611
0.28	0.23245	0.06897	0.85423
0.29	0.22123	0.06509	0.86191
0.30	0.21048	0.06145	0.86919

TABLE(5.2)

DISSYMMETRY OF THE CONCENTRATION PROFILE  
(A = 2,  $\Delta\tau = 0.0005$ ,  $\Delta X = 0.05$ )

Dimensionless time (TAU)	Dimensionless Concentration (C)		Fraction Extracted (Em)
	X = -0.8	X = +0.8	
0.002	0.99854	0.99834	0.11237
0.004	0.95946	0.95517	0.14930
0.006	0.90843	0.89865	0.17768
0.008	0.85958	0.84442	0.20154
0.010	0.81554	0.79549	0.22246
0.012	0.77636	0.75196	0.24128
0.014	0.74153	0.71326	0.25848
0.016	0.71043	0.67873	0.27439
0.018	0.68251	0.64776	0.28925
0.02	0.65730	0.61983	0.30321
0.04	0.49330	0.43971	0.41232
0.06	0.40405	0.34400	0.49120
0.08	0.34481	0.28231	0.55407
0.10	0.30095	0.23818	0.60650
0.11	0.28263	0.22029	0.62976
0.12	0.26606	0.20445	0.65137
0.13	0.25091	0.19028	0.67152
0.14	0.23693	0.17749	0.69035
0.15	0.22394	0.16537	0.70800
0.16	0.21180	0.15525	0.72456
0.17	0.20041	0.14549	0.74012
0.18	0.18968	0.13648	0.75475
0.19	0.17956	0.12815	0.76852
0.20	0.16999	0.12041	0.78150
0.21	0.16094	0.11322	0.79372
0.22	0.15236	0.10650	0.80525
0.23	0.14422	0.10024	0.81612
0.24	0.13613	0.09437	0.82688
0.25	0.12919	0.08888	0.83606
0.26	0.12226	0.08374	0.84519
0.27	0.11568	0.07891	0.85381
0.28	0.10944	0.07438	0.86195
0.29	0.10353	0.07012	0.86963
0.30	0.09792	0.06611	0.87688

TABLE(5.3)

DISSYMMETRY OF THE CONCENTRATION PROFILE(A = 4,  $\Delta\tau = 0.0005$ ,  $\Delta X = 0.05$ )

Dimensionless time (TAU)	Dimensionless Concentration (C)		Fraction Extracted ( $\bar{m}$ )
	X = -0.8	X = +0.8	
0.002	0.99845	0.99837	0.11237
0.004	0.95755	0.95569	0.14930
0.006	0.90407	0.89984	0.17768
0.008	0.85284	0.84627	0.20154
0.01	0.80664	0.79794	0.22247
0.012	0.76555	0.75495	0.24129
0.014	0.72902	0.71673	0.25850
0.016	0.69643	0.68264	0.27442
0.018	0.66718	0.65206	0.28928
0.02	0.64079	0.62447	0.30324
0.04	0.46997	0.44646	0.41244
0.06	0.37814	0.35170	0.49141
0.08	0.31806	0.29044	0.55439
0.1	0.27424	0.24543	0.60693
0.11	0.25617	0.22852	0.63024
0.12	0.23997	0.21261	0.65190
0.13	0.22528	0.19834	0.67210
0.14	0.21184	0.18541	0.69099
0.15	0.19945	0.17361	0.70868
0.16	0.18797	0.16279	0.72528
0.17	0.17728	0.15282	0.74088
0.18	0.16728	0.14358	0.75555
0.19	0.15791	0.13500	0.76936
0.20	0.14911	0.12701	0.78237
0.21	0.14082	0.11956	0.79462
0.22	0.13302	0.11258	0.80618
0.23	0.12565	0.10605	0.81707
0.24	0.11870	0.09992	0.82734
0.25	0.11214	0.09418	0.83703
0.26	0.10593	0.08877	0.84617
0.27	0.10036	0.08370	0.85438
0.28	0.09454	0.07892	0.86294
0.29	0.08930	0.07443	0.87063
0.30	0.08435	0.07020	0.87788

TABLE(5.4)

## ANALYTICAL AND NUMERICAL SOLUTION FOR A CYLINDER

Dimensionless Time (TAU)	Dimensionless Concentration (C)		Fraction Extracted (Em)	
	Analytical	Numerical	Analytical	Numerical
0.002	0.99825	0.99840	0.09891	0.11237
0.004	0.97163	0.95643	0.013868	0.14930
0.006	0.92399	0.90152	0.16872	0.17768
0.008	0.87249	0.84888	0.19371	0.20154
0.010	0.82376	0.80140	0.21547	0.22247
0.012	0.77953	0.75917	0.23495	0.24130
0.014	0.73990	0.72163	0.25268	0.25850
0.018	0.67260	0.65809	0.28428	0.28929
0.02	0.74393	0.63099	0.29856	0.30325
0.04	0.46053	0.45591	0.40960	0.41247
0.06	0.36428	0.36237	0.48943	0.49148
0.08	0.30243	0.30162	0.55292	0.55448
0.10	0.25803	0.25773	0.60582	0.60706
0.11	0.23992	0.23977	0.62927	0.63038
0.12	0.22380	0.22376	0.65106	0.65206
0.13	0.20929	0.20952	0.67137	0.67228
0.14	0.19610	0.19619	0.69036	0.69118
0.15	0.18403	0.18416	0.70814	0.70888
0.16	0.17292	0.17307	0.72482	0.72550
0.17	0.16263	0.16281	0.74049	0.74111
0.18	0.15307	0.15326	0.75522	0.75580
0.19	0.14416	0.14436	0.76909	0.76961
0.20	0.13583	0.13604	0.78215	0.78263
0.21	0.12803	0.12824	0.79445	0.79489
0.22	0.12072	0.12092	0.80605	0.80645
0.23	0.11384	0.11404	0.81698	0.81735
0.24	0.10738	0.10757	0.82729	0.82763
0.25	0.10130	0.10149	0.83701	0.83732

TABLE(5.5)

DISSYMMETRY OF THE CONCENTRATION PROFILE $(A = 1, \Delta\tau = 0.0003, \Delta X = 0.04)$ 

Dimensionless time (TAU)	Dimensionless Concentration (C)		Fraction Extracted (Em)
	X = -0.8	X = +0.8	
0.006	0.95931	0.90402	0.17520
0.012	0.89328	0.75474	0.23923
0.018	0.84102	0.64683	0.28733
0.06	0.64175	0.33391	0.48829
0.12	0.49263	0.19306	0.64613
0.15	0.43436	0.15508	0.70174
0.18	0.38152	0.12672	0.74767
0.21	0.33338	0.10471	0.78606
0.24	0.28985	0.08718	0.81806

TABLE(5.6)

DISSYMMETRY OF THE CONCENTRATION PROFILE $(A = 2, \Delta\tau = 0.0003, \Delta X = 0.04)$ 

Dimensionless Time (TAU)	Dimensionless Concentration (C)		Fraction Extracted ( $\bar{E}_m$ )
	X = -0.8	X = +0.8	
0.006	0.91510	0.90555	0.17528
0.012	0.78344	0.75874	0.23947
0.018	0.68804	0.65263	0.28778
0.06	0.40542	0.34443	0.49058
0.12	0.26657	0.20430	0.65105
0.15	0.22431	0.16568	0.70776
0.18	0.18998	0.13630	0.75455
0.21	0.16118	0.11305	0.79357
0.24	0.13672	0.09422	0.82625

TABLE(5.7)

DISSYMMETRY OF THE CONCENTRATION PROFILE(A = 4,  $\Delta\gamma = 0.0003$ ,  $\Delta X = 0.04$ )

Dimensionless Time (TAU)	Dimensionless Concentration (C)		Fraction Extracted (Em)
	X = -0.8	X = +0.8	
0.006	0.91084	0.90671	0.17528
0.012	0.77247	0.76176	0.23949
0.018	0.67238	0.65699	0.28782
0.06	0.57904	0.35223	0.49080
0.12	0.24013	0.21252	0.65160
0.15	0.19953	0.17347	0.70845
0.18	0.16732	0.14344	0.75538
0.21	0.14084	0.11942	0.79448
0.24	0.11871	0.09980	0.82723

TABLE(5.8)

DIFFERENCE IN THE DIMENSIONLESS CONCENTRATION AT X = 70.8

TAU \ A	1.0	2.0	4.0
0.01	0.11033	0.02005	0.00370
0.1	0.29635	0.06177	0.02781
0.2	0.22834	0.04958	0.02210



TABLE(5.9)

FRACTION EXTRACTED FOR A TORUS AND A CYLINDER

TAU	A = 1.0	A = 2.0	A = 4.0	Cylinder
0.01	0.22233	0.22246	0.22247	0.22247
0.04	0.41110	0.41232	0.41244	0.41247
0.1	0.60270	0.60650	0.60693	0.60706
0.15	0.70233	0.70800	0.70868	0.70888
0.2	0.77454	0.78150	0.78237	0.78263
0.25	0.82845	0.83606	0.83703	0.83732

TABLE(5.10)

CONCENTRATION AT THE CENTER OF THE TORUS

TAU	DIMENSIONLESS CONCENTRATION (C)		
	A = 1	A = 2	A = 4
0.02	1.0000	1.0000	1.0000
0.04	0.9966	0.9963	0.9962
0.05	0.9879	0.9871	0.9869
0.10	0.8566	0.8485	0.8472
0.12	0.7851	0.7736	0.7717
0.14	0.7137	0.6993	0.6970
0.16	0.6456	0.6288	0.6261
0.18	0.5823	0.5636	0.5607

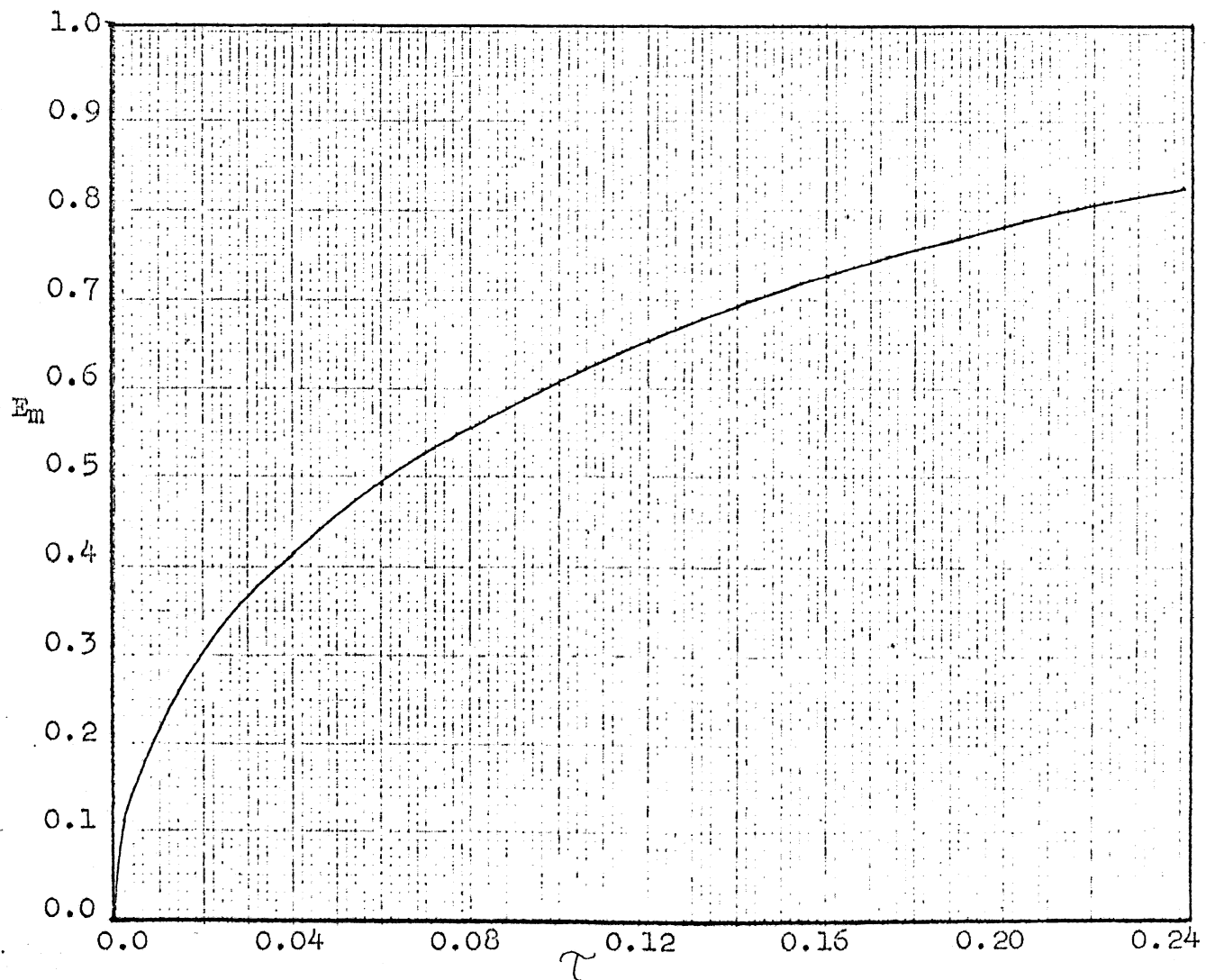


Figure 5.1 Fraction Extracted Versus Dimensionless Time

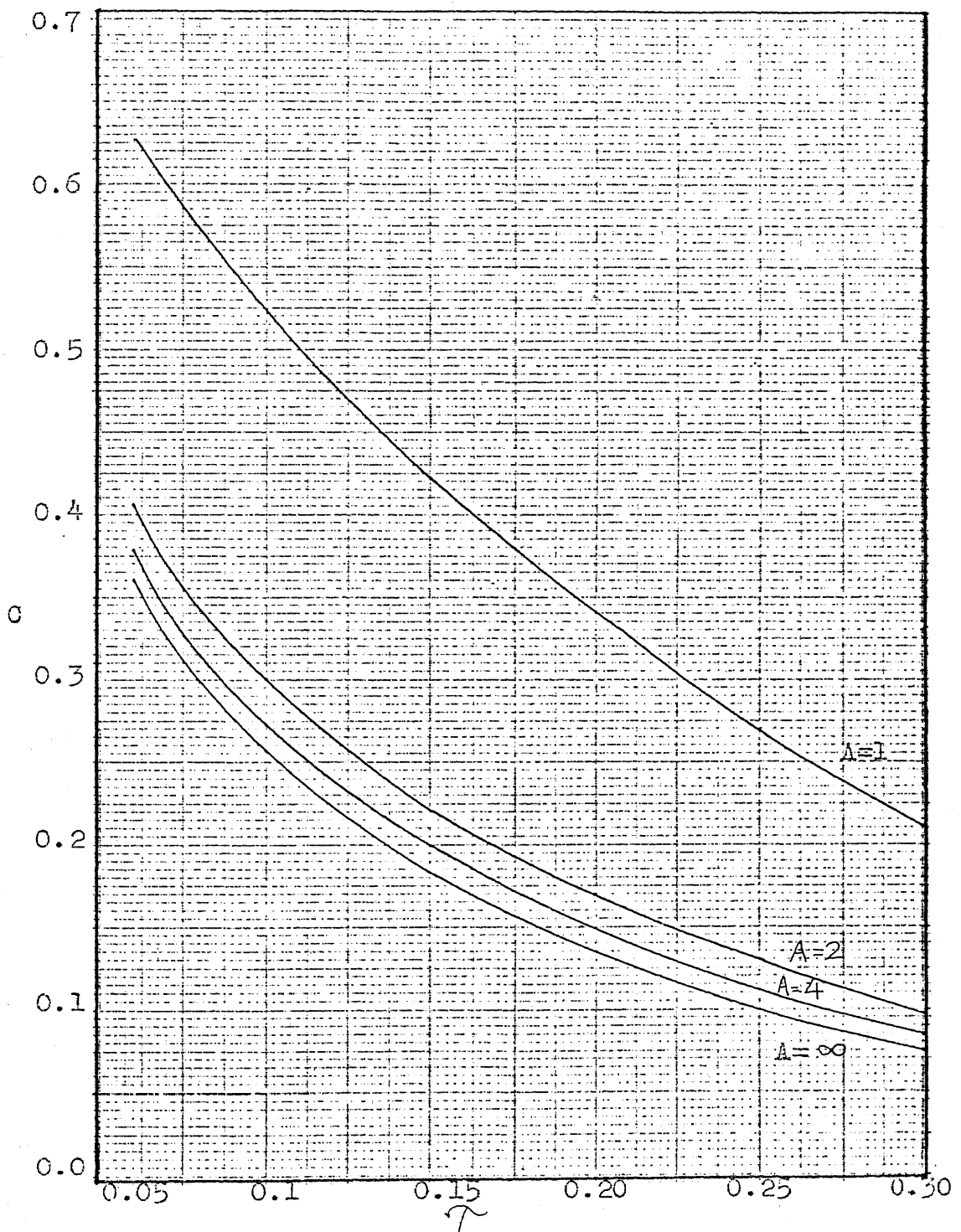


Figure 5.2 Dimensionless Concentration at  $X = - 0.8$  Versus Dimensionless Time

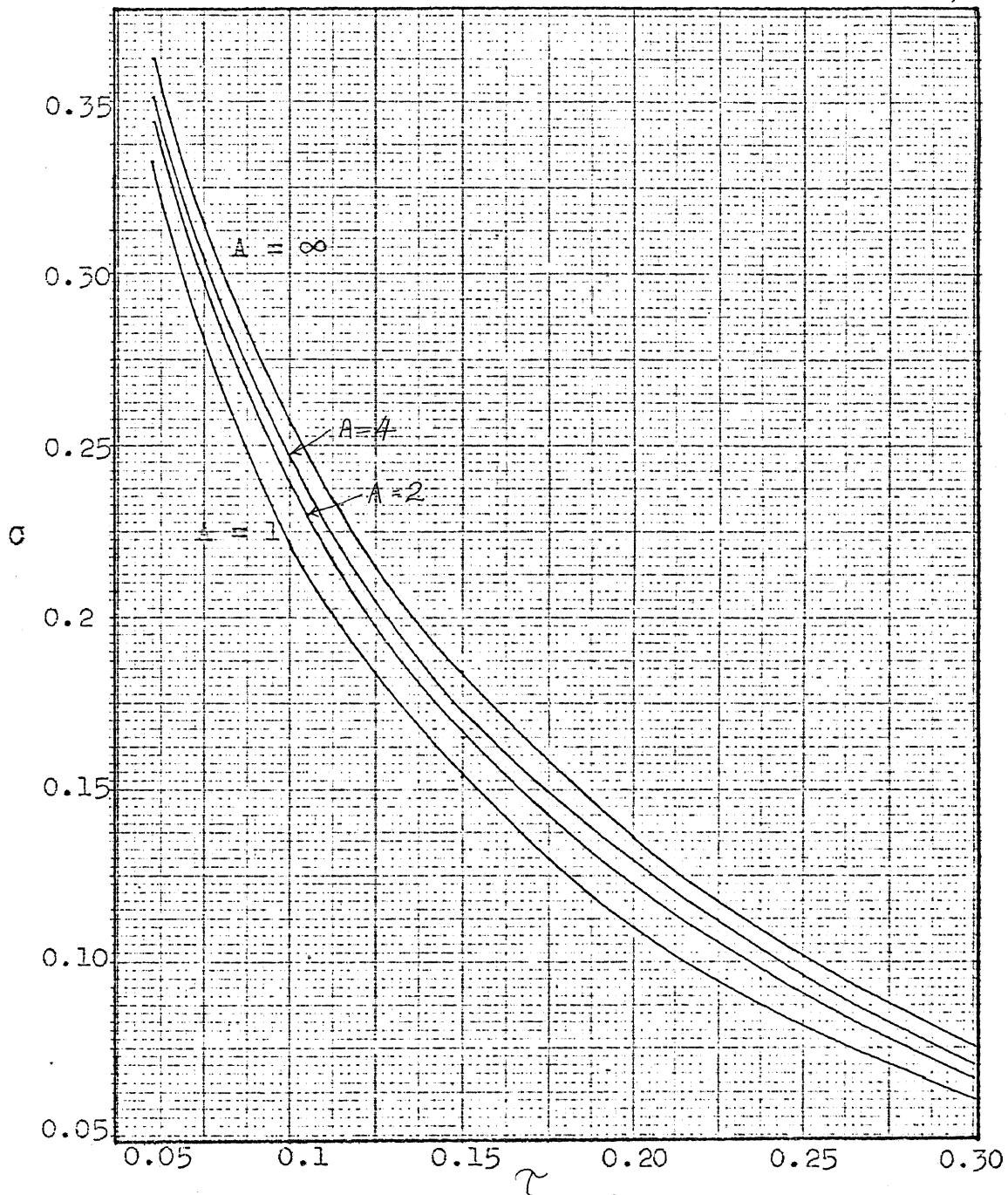


Figure 5.3 Dimensionless Concentration at  $X = +0.8$  Versus Dimensionless Time

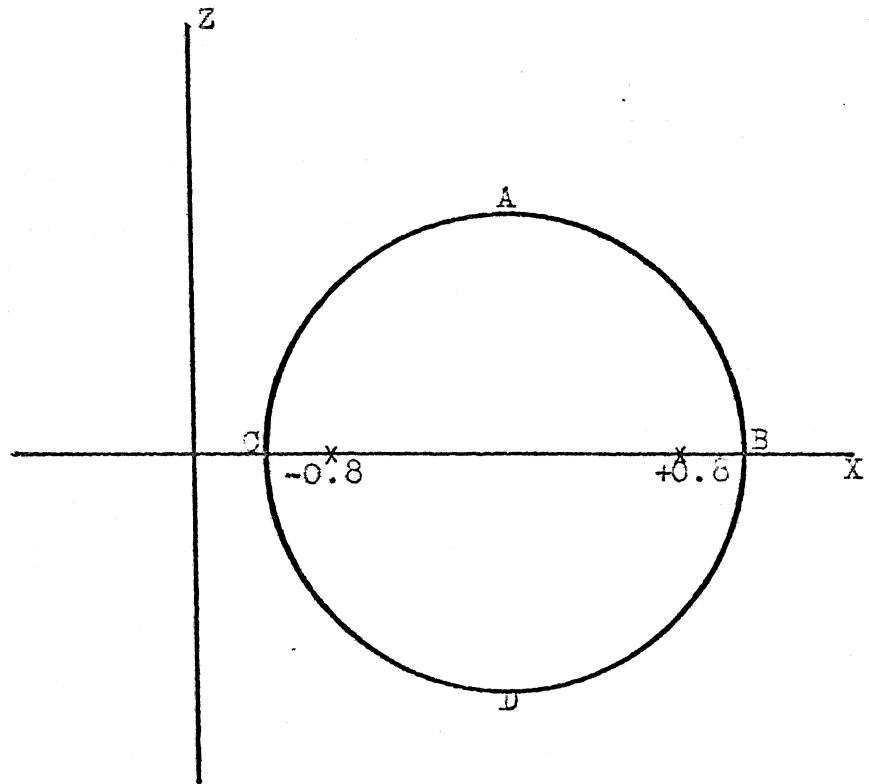


Figure 5.4 Part of the Cross Section of the Torus

## VI. CONCLUSIONS

The partial differential equation for molecular diffusion into a torus is derived in this study. This equation reduces to special cases for the two extreme values of the parameter A. For  $A = 0$ , it describes molecular diffusion into a sphere and for  $A = \infty$ , it reduces to the case of an infinite cylinder. The partial differential equation is solved by the explicit finite difference method for the values of  $A = 1, 2, 4, \text{ and } \infty$ . The finite difference equation is stable for  $\frac{\Delta\tau}{(\Delta X)^2} \leq \frac{1}{4}$ ; it is unstable for  $\frac{\Delta\tau}{(\Delta X)^2} > \frac{1}{4}$ .

The following conclusions are presented from an analysis of the results:

(1) The concentration profile is symmetrical about both the coordinate axes (X and Z) for molecular diffusion into a sphere and cylinder, but the parameter A appearing in the partial differential equation for the torus results in a dissymmetry of the concentration profile about the Z-axis.

(2) The torus curvature (i.e., the magnitude of the parameter A) affects the concentration profile within the torus. For small values of A, the effect of the curvature is significant and hence the values of the point concentrations vary widely from concentrations in a cylinder. (For example, at  $X = -0.8$  and  $\tau = 0.1$ , the variations in the point concentrations are 15.6% and

6.28% for  $A = 2$  and  $A = 4$ , respectively). When  $A$  is large, the concentration profile tends to be symmetrical; and for very large  $A$ , the values of concentrations in the torus correspond almost exactly to those for a cylinder.

(3) The fraction extracted (which is related to the average concentration of the solute in the torus) at various values of the dimensionless time is independent of the parameter  $A$ . This appears to be consistent with the physical situation. The value of the point concentration in a cylinder for a given radius is between the two values of the point concentration at diametrically opposite points (along  $X$  axis) in a torus.

(4) The effect of diffusion in  $\Theta$  direction on the point concentration and the fraction extracted is negligible in comparison to radial direction.

(5) The assumption that the effect of the torus curvature is negligible in the eddy diffusion model of Handlos and Baron, may be justified.



VII. APPENDICES

APPENDIX ADiffusion Equation

For a torus (11)

$$X = (a + r \sin \theta) \cos \phi \quad (3.11)$$

$$Y = (a + r \sin \theta) \sin \phi \quad (3.12)$$

$$Z = r \cos \theta \quad (3.13)$$

and

$$(ds)^2 = (dx)^2 + (dy)^2 + (dz)^2 \quad (A.1)$$

$$dx = -(a + r \sin \theta) \sin \phi d\phi + \cos \phi (r \cos \theta d\theta + dr \sin \theta) \quad (A.2)$$

$$dy = (a + r \sin \theta) \cos \phi d\phi + \sin \phi (r \cos \theta d\theta + dr \sin \theta) \quad (A.3)$$

$$dz = -r \sin \theta d\theta + dr \sin \theta \quad (A.4)$$

so that

$$(ds)^2 = (dr)^2 + r^2 (d\theta)^2 + (a + r \sin \theta)^2 (d\phi)^2 \quad (A.5)$$

Comparing equation (A.5) with

$$(ds)^2 = h_1 (du_1)^2 + h_2 (du_2)^2 + h_3 (du_3)^2 \quad (A.6)$$

$$h_1 = 1 \quad (A.7)$$

$$h_2 = r \quad (A.8)$$

$$h_3 = (a + r \sin \theta) \quad (A.9)$$

Therefore

$$\nabla^2 C_A = \frac{1}{r(a+r \sin \theta)} \left\{ \frac{\partial}{\partial r} \left[ r(a+r \sin \theta) \frac{\partial C_A}{\partial r} \right] + \frac{\partial}{\partial \theta} \left[ \frac{(a+r \sin \theta)}{r} \frac{\partial C_A}{\partial \theta} \right] + \frac{\partial}{\partial \phi} \left[ \frac{r}{(a+r \sin \theta)} \frac{\partial C_A}{\partial \phi} \right] \right\} \quad (A.10)$$

and Fick's second law of molecular diffusion is given by

$$\frac{\partial C_A}{\partial t} = D_{AB} \nabla^2 C_A \quad (A.11)$$

where  $\nabla^2 C_A$  is expressed by equation (A.10)

APPENDIX BNumerical Solution of Equation (4.21)

$$\bar{C}(\tau_k) = \frac{4\pi \int_{-1}^1 (A+x) dx \int_0^{\sqrt{1-x^2}} c(x,z,\tau) dz}{2\pi^2 A} \quad (4.21)$$

Let  $F(x, \tau_k) = \int_0^{\sqrt{1-x^2}} c(x,z,\tau_k) dz$  (B.1)

so that

$$\bar{C}(\tau_k) = \frac{2}{\pi A} \int_{-1}^1 (A+x) F(x, \tau_k) dx \quad (B.2)$$

Introducing the trapezoidal rule as the quadrature formula for the evaluation of integrals

$$\begin{aligned} F(x_i, \tau_k) &= \int_0^{\sqrt{1-x_i^2}} c(x_i, z, \tau_k) dz \\ &= \frac{\Delta X}{2} (c_{i,1,k} + 2c_{i,2,k} + \dots + c_{i,B-1,k}) \\ &\quad + \frac{h_{iu}}{2} (c_{i,B-1,k} + c_{i,B,k}) \end{aligned} \quad (B.3)$$

where

B-1 denotes the point next to the boundary

B denotes the point on the boundary

$h_{iu}$  is the distance between these two points in the Z direction.

Thus

$$C(\tau_k) = \frac{2}{\pi A} \frac{\Delta X}{2} \left[ (A+x_1) F(x_1, \tau_k) + 2(A+x_2) F(x_2, \tau_k) + \dots \right. \\ \left. \dots + 2(A+x_{B-1}) F(x_{B-1}, \tau_k) + (A+x_B) F(x_B, \tau_k) \right]$$

(B.4)

APPENDIX C

Analytical Solution For A Cylinder

Equation (3.20a) for diffusion into a torus reduces to that for a cylinder when  $A \rightarrow \infty$ . Molecular diffusion equation for an infinite cylinder is

$$\frac{\partial C_A}{\partial t} = \frac{1}{r} \frac{\partial}{\partial r} \left( r D \frac{\partial C_A}{\partial r} \right) \quad (\text{C.1a})$$

with the following boundary conditions

$$C_A = C_{A_1} \quad r = r_i \quad t \geq 0 \quad (\text{C.1b})$$

$$C_A = C_{A_0} \quad 0 \leq r < r_i \quad t = 0 \quad (\text{C.1c})$$

The analytical solution of equation (C.1a) with its boundary conditions is given by (2).

$$\frac{C_A - C_{A_1}}{C_{A_0} - C_{A_1}} = \frac{2}{r_i} \sum_{n=1}^{\infty} e^{-D\alpha_n^2 t} \frac{J_0(r\alpha_n)}{J_1(r_i\alpha_n)} \quad (\text{C.2})$$

where  $\alpha_n$  are the roots of

$$J_0(r_i\alpha_n) = 0 \quad (\text{C.3})$$

Let  $r_i\alpha_n = \beta_n$  (C.4)

$$\frac{r}{r_i} = R \quad (\text{C.5})$$

$$\frac{D t}{r_i^2} = \gamma \quad (\text{C.6})$$

and

$$\frac{C_A - C_{A_1}}{C_{A_0} - C_{A_1}} = C \quad (\text{C.7})$$

Then equation (C.2) transforms into

$$C = 2 \sum_{n=1}^{\infty} e^{-\beta_n^2 \gamma} \frac{J_0(R\beta_n)}{\beta_n J_1(\beta_n)} \quad (\text{C.8})$$

Thus from equation (C.8), the dimensionless concentration can be determined for the various values of  $R$  and  $\gamma$ .

The formula for the dimensionless volumetric average concentration is derived from equation (C.8) and it is

given by

$$\bar{C}(\tau) = 4 \sum \frac{e^{-\beta_n^2 \tau}}{\beta_n^2} \quad (0.9)$$

The computer programs are written for the calculation of the point concentration and volumetric average concentration from equations (0.8) and (0.9) respectively. Forty values of  $\beta_n$  are reported in (14).

LEVEL: 1JUL66

IBM OS/360 BASIC FORTRAN IV (E) COMPILATION

```
      CCC      ANALYTICAL SOLUTION FOR DIFFUSION TO A CYLINDER
      C      CALCULATION OF POINT CONCENTRATION
S.0001      DIMENSION A(40),R(40),R1(40)
S.0002      READ(1,200)(A(J),J=1,40)
S.0003      WRITE(3,101)
S.0004      DO 20 J=1,40
S.0005          X=A(J)*0.8
S.0006          N=0.0
S.0007          CALL RESJ (X,N,BESS,.00005,IER)
S.0008      20  R(J)=BESS
S.0009          DO 30 J=1,40
S.0010          X=A(J)
S.0011          N=1
S.0012          CALL RESJ (X,N,BESS,.00005,IER)
S.0013      30  R1(J)=BESS
S.0014          DTA=0.0005
S.0015          DO 10 K=1,600
S.0016          TAU=DTA*K
S.0017          SUM=0.0
S.0018          DO 40 J=1,40
S.0019          P=A(J)
S.0020          IF(P**2*TAU-170.)40,10,10
S.0021      40  SUM=SUM+2.*R(J)/(R1(J)*EXP((P**2)*TAU)*P)
S.0022      10  WRITE(3,100)TAU,SUM
S.0023      100 FORMAT(10X,F15.5,E18.8)
S.0024      101 FORMAT(/25X,'TAU',5X,'MESH POINT')
S.0025      200 FORMAT(F15.5)
S.0026      END
```

LEVEL: 1JUL66 IRM OS/360 BASIC FORTRAN IV (E) COMPILATION

CCC	ANALYTICAL SOLUTION FOR DIFFUSION TO A CYLINDER CALCULATION OF FRACTION EXTRACTED
S.0001	DOUBLE PRECISION A(40)
S.0002	DQURLF PRECISION TAU, SUM, B, DTA, P, FE
S.0003	PFA0(1, 200)(A(J), J=1, 40)
S.0004	DTA=0.0005
S.0005	DO 11 K=1, 700
S.0006	TAU=DTA*K
S.0007	SUM=0.0
S.0008	DO 20 J=1, 40
S.0009	R=A(J)
S.0010	IF (R**2*TAU-100.0) 21, 10, 10
S.0011	P=DEXP((R**2)*TAU)*(R**2)
S.0012	21 SUM=SUM+4.0/P
S.0013	10 FE=1.0-SUM
S.0014	11 WRITE(3, 100)TAU, FE
S.0015	100 FORMAT(10X, F15.5, 10X, F15.5)
S.0016	200 FORMAT(F18.8)
S.0017	END

APPENDIX D

Truncation Error

Expand each term of equation (4.23) by Taylor's series (8). The argument of  $C$  in right side of the equation is  $(I, J, K)$ .

$$C(I, J, K+1) = C + \frac{\partial C}{\partial \tau} \Delta \tau + \frac{\partial^2 C}{\partial \tau^2} \frac{(\Delta \tau)^2}{2!} \quad (D.1)$$

$$C(I+1, J, K) = C + \frac{\partial C}{\partial X} \Delta X + \frac{\partial^2 C}{\partial X^2} \frac{(\Delta X)^2}{2!} + \frac{\partial^3 C}{\partial X^3} \frac{(\Delta X)^3}{3!} + \frac{\partial^4 C}{\partial X^4} \frac{(\Delta X)^4}{4!} \quad (D.2)$$

$$C(I-1, J, K) = C - \frac{\partial C}{\partial X} \Delta X + \frac{\partial^2 C}{\partial X^2} \frac{(\Delta X)^2}{2!} - \frac{\partial^3 C}{\partial X^3} \frac{(\Delta X)^3}{3!} + \frac{\partial^4 C}{\partial X^4} \frac{(\Delta X)^4}{4!} \quad (D.3)$$

$$C(I, J+1, K) = C + \frac{\partial C}{\partial Z} \Delta Z + \frac{\partial^2 C}{\partial Z^2} \frac{(\Delta Z)^2}{2!} + \frac{\partial^3 C}{\partial Z^3} \frac{(\Delta Z)^3}{3!} + \frac{\partial^4 C}{\partial Z^4} \frac{(\Delta Z)^4}{4!} \quad (D.4)$$

$$C(I, J-1, K) = C - \frac{\partial C}{\partial Z} \Delta Z + \frac{\partial^2 C}{\partial Z^2} \frac{(\Delta Z)^2}{2!} - \frac{\partial^3 C}{\partial Z^3} \frac{(\Delta Z)^3}{3!} + \frac{\partial^4 C}{\partial Z^4} \frac{(\Delta Z)^4}{4!} \quad (D.5)$$

Since a square mesh is used,  $\Delta X = \Delta Z$

Substitute these terms in equation (4.23) and let

$$P = \frac{1}{A+X} \frac{S \cdot \Delta X}{2}$$

so that

$$\begin{aligned} C \frac{\partial C}{\partial \tau} \Delta \tau + \frac{\partial^2 C}{\partial \tau^2} \frac{(\Delta \tau)^2}{2!} &= (S+P) \left[ C + \frac{\partial C}{\partial X} \Delta X + \frac{\partial^2 C}{\partial X^2} \frac{(\Delta X)^2}{2!} + \frac{\partial^3 C}{\partial X^3} \frac{(\Delta X)^3}{3!} + \frac{\partial^4 C}{\partial X^4} \frac{(\Delta X)^4}{4!} \right] + \\ & (S-P) \left[ C - \frac{\partial C}{\partial X} \Delta X + \frac{\partial^2 C}{\partial X^2} \frac{(\Delta X)^2}{2!} - \frac{\partial^3 C}{\partial X^3} \frac{(\Delta X)^3}{3!} + \frac{\partial^4 C}{\partial X^4} \frac{(\Delta X)^4}{4!} \right] \\ & + (S) \left[ C + \frac{\partial C}{\partial Z} \Delta Z + \frac{\partial^2 C}{\partial Z^2} \frac{(\Delta Z)^2}{2!} + \frac{\partial^3 C}{\partial Z^3} \frac{(\Delta Z)^3}{3!} + \frac{\partial^4 C}{\partial Z^4} \frac{(\Delta Z)^4}{4!} \right] \\ & + (S) \left[ C - \frac{\partial C}{\partial Z} \Delta Z + \frac{\partial^2 C}{\partial Z^2} \frac{(\Delta Z)^2}{2!} - \frac{\partial^3 C}{\partial Z^3} \frac{(\Delta Z)^3}{3!} + \frac{\partial^4 C}{\partial Z^4} \frac{(\Delta Z)^4}{4!} \right] \\ & + (1-4S)C + T_{ij} \Delta \tau \end{aligned} \quad (D.6)$$

This on simplification gives

$$\begin{aligned} \frac{\partial C}{\partial \tau} \Delta \tau + \frac{\partial^2 C}{\partial \tau^2} \frac{(\Delta \tau)^2}{2!} &= 2P \Delta X \frac{\partial C}{\partial X} + S(\Delta X)^2 \frac{\partial^2 C}{\partial X^2} + \frac{1}{3} P(\Delta X)^3 \frac{\partial^3 C}{\partial X^3} \\ & + \frac{1}{6} S(\Delta X)^4 \frac{\partial^4 C}{\partial X^4} + S(\Delta X)^2 \frac{\partial^2 C}{\partial Z^2} + \frac{1}{12} S(\Delta X)^4 \frac{\partial^4 C}{\partial Z^4} + T_{ij} \Delta \tau \end{aligned} \quad (D.7)$$



From equation (3.23a)

$$\frac{\partial c}{\partial \gamma} \Delta \gamma = S(\Delta X)^2 \frac{\partial^2 c}{\partial X^2} + S(\Delta X)^2 \frac{\partial^2 c}{\partial Z^2} + 2P \Delta X \frac{\partial c}{\partial X} \quad (D.8)$$

Therefore (D.7) becomes

$$\frac{\partial^2 c}{\partial \gamma^2} \frac{(\Delta \gamma)^2}{2!} = \frac{1}{3} P(\Delta X)^3 \frac{\partial^3 c}{\partial X^3} + \frac{1}{12} S(\Delta X)^4 \frac{\partial^4 c}{\partial X^4} + \frac{1}{12} S(\Delta X)^4 \frac{\partial^4 c}{\partial Z^4} + T_{ij} \Delta \gamma \quad (D.9)$$

Substituting the values of S, P and rearranging the terms, truncation error is given by

$$T_{ij} = \frac{1}{2} \Delta \gamma \frac{\partial^2 c}{\partial \gamma^2} - \frac{1}{6(A+X)} (\Delta X)^2 \frac{\partial^3 c}{\partial X^3} - \frac{1}{12} (\Delta X)^2 \left( \frac{\partial^4 c}{\partial X^4} + \frac{\partial^4 c}{\partial Z^4} \right) \quad (D.10)$$

Thus

$$T_{ij} = O(\Delta \gamma) + O(\Delta X)^2 \quad (D.11)$$

## APPENDIX E

### Computer Program For The Numerical Solution

The computer program listed in this appendix has each line numbered on the left side of the program. The program is explained by reference to these numbers and the grid work presented in Figure E.1. It is designed to run on the IBM model 360 computer. The language is in Fortran IV.

### Explanation of the Computer Program

This program is written for solving equation (3.23a) by the finite difference method. The overall procedure for calculation is to proceed from  $Z=0$  to  $Z=\sqrt{1-x^2}$  for each value of  $x$  varying between  $-1$  to  $+1$ . In the following explanation, it is assumed that  $\Delta X=0.05$ ,  $\Delta \tau=0.0005$ ,  $C(X, Z, 0)=1$  and  $C(X, \pm\sqrt{1-x^2}, \tau)=0$ .

Lines 1 through 4 dimension and double precision the program variables.

Lines 8 through 12 define the essential central variables.  $A1=A$ ;  $DTA=\Delta \tau$ ;  $DX=\Delta X$ ;  $BC$  = boundary condition on the surface;  $PI$  = initial concentration in the torus.

Lines 13 through 16 represent the constant terms of the finite difference equations.

Lines 17 through 20 are the terms which control various DO loops.  $NT$  = number of time steps;  $NX$  = number of spatial increments in the X direction

(  $NX = 40$  for  $X = 0.05$  );  $NZ = NX + 1$ ;  $NZ =$  number that locates nodal points along  $Z=0$  line.

Lines 21 through 45 calculate the location of the nodal points, stores the values of  $X$  and  $Z$  at each nodal point and on the boundary. It also defines the initial concentration profile.

Lines 25 through 35 contain the routine for locating the upper nodes on each line of constant  $X$ . The key to the node location routine is storing a floating point number in a fixed point location and taking advantage of the round off. In line 28 the factor of  $5 \times 10^{-5}$  had to be used to compensate for computer round off error when calculating a floating point number.

In all parts of the program,  $I$  corresponds to the  $X$  direction and  $J$  to the  $Z$  direction. In the overall scheme of the solution two time planes, denoted as  $C(I,J)$  and  $B(I,J)$ , are used. Initially,  $C(I,J)$  is stored and then by classical explicit method  $B(I,J)$  is calculated. Then, the values of  $B(I,J)$  are stored in  $C(I,J)$  locations and  $C(I,J)$  is printed out and another  $B(I,J)$  set is calculated.

Lines 47 through 86 is the explicit method calculation of the concentrations at all points. Line 47 is the DO loop for time steps. Line 48 is the loop for steps from  $Z=0$  to  $Z=\sqrt{1-X^2}$  for each value of  $X$ . Lines 53 and 54 test the node to see if it has an unequal increment. In lines 57 and 58,  $ALX$  and  $ALZ$  are the distances, number

of increments between the nodes  $(I \pm 1, J)$  or  $(I, J - 1)$  and boundary through the node  $(I, J)$ . Line 59 determines whether ALX or ALZ is larger. Line 67 tests whether X is negative or positive. Line 69 calculates the concentration at the points for negative X and ALX less than ALZ. Line 75 calculates the concentrations at the points for ALZ less than ALX. Line 80 calculates the concentration at the points on  $Z=0$  line. Line 83 calculates the concentrations for the ES set of points.

Lines 87 through 101 calculate the dimensionless volumetric average concentration using the trapezoidal rule for double integration.

Line 102 defines the fraction extracted. Line 103 prints out the value of the previous  $\tau$ , point concentration at  $Z=0$  and  $X=-0.8$  and fraction extracted at the corresponding value of  $\tau$ .

Lines 104 to 110 switch the values  $B(I, J)$  to  $C(I, J)$  for calculations at the next time step.

Line 111 defines the next time step. Line 112 is the end of the time DO loop.

For the numerical solution to the diffusion equation of a cylinder, the following changes in the program are necessary.

$$A1 = 0, \quad SCL = 0, \quad B3 = \frac{2 \cdot DX}{\tau}, \quad STF = STF + PXT(I)$$

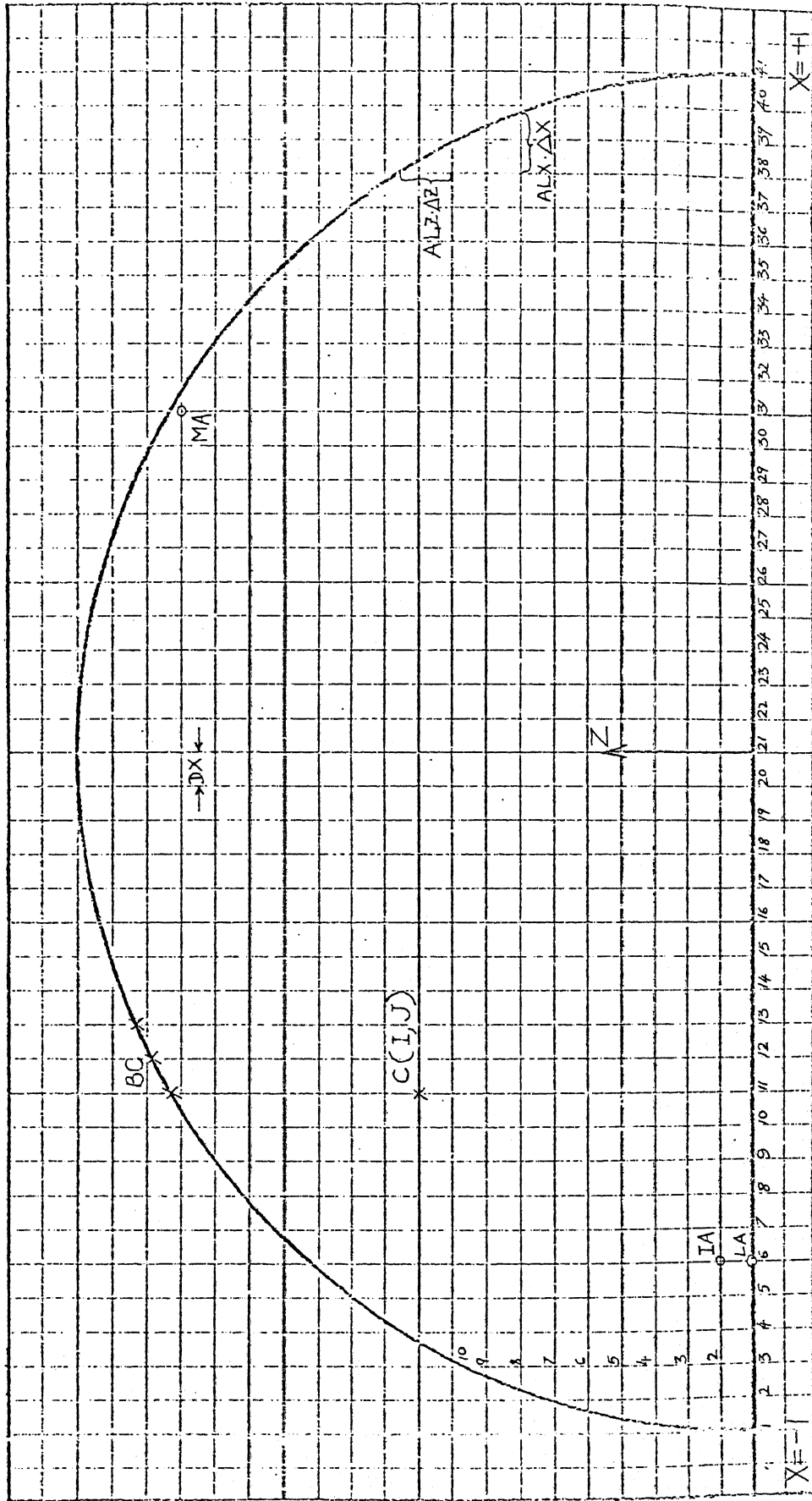


Figure E.1 Network for Symbols Used in the Computer Program

LEVEL: 1JUL66

IBM OS/360 BASIC FORTRAN IV (E) COMPILATION

```

C      MASS TRANSFER FROM A TORUS
C      SOLUTION IN RECTANGULAR COORDINATES BY EXPLICIT METHOD
S.0001  DOUBLE PRECISION C(41,21),B(41,21),X(41),Z(41,21),M(41)
S.0002  DOUBLE PRECISION DTA,DX,BC,PI,S,S2,SC1,S4,AN,ANN
S.0003  DOUBLE PRECISION FXT(41),STF,B3,CAV,SUMF
S.0004  DOUBLE PRECISION TAU,A1,ALX,ALZ,TH,FE
S.0005  WRITE(3,101)
S.0006      100  FORMAT(710X,F15.5,15X,F15.5,15X,F15.5,5X,F10.5)
S.0007      101  FORMAT(17X,'TAU',25X,'MESH POINT',25X,'FE',5X,'MESH POINT')
CCC     PHYSICAL AND MATHEMATICAL CONTROL VARIABLES
S.0008      A1=2.000000
S.0009      DTA=0.0005
S.0010      DX=0.05
S.0011      BC=0.0
S.0012      PI=1.0
CCC     CALCULATION OF CONSTANT TERMS
S.0013      S=DTA/(DX**2)
S.0014      S2=S*DX/2.
S.0015      S4=(1.-4.*S)
S.0016      B3=(1.0/(3.14159265*A1))*DX*2.0
CCC     NESTING CONTROL CONSTANTS
S.0017      NT=600
S.0018      NX=2/DX
S.0019      MZ=NX+1
S.0020      N7=1
CCC     CALCULATION OF NESTING INDICES AND STORAGE OF INITIAL CONDITIONS
S.0021      C(I,N7)=BC
S.0022      C(MZ,NZ)=BC
S.0023      X(2)=-0.95
S.0024      DO 1 I=2,NX
S.0025      AN=DSQRT(1.-(X(I)**2))/DX
S.0026      N=AN
S.0027      ANN=N
S.0028      IF(AN-ANN-5.0E-5)2,2,3
S.0029      2  CONTINUE
S.0030      M(I)=N7+N
S.0031      GO TO 4
S.0032      3  CONTINUE
S.0033      M(I)=N7+N+1
S.0034      4  CONTINUE
S.0035      MB=M(I)

```

```

S.0036      C(I,MB)=BC
S.0037      Z(I,MB)=DSQRT(1.-X(I)**2)
S.0038      LA=NZ
S.0039      MA=M(I)-1
S.0040      DO 6 J=LA,MA
S.0041      C(I,J)=PI
S.0042      Z(I,J)=(J-NZ)*DX
S.0043      6 CONTINUE
S.0044      X(I+1)=(I-20)*DX
S.0045      1 CONTINUE
CCC 1 CALCULATION OF CONCENTRATION PROFILES
S.0046      TAU=0.0
S.0047      DO 70 KK=1,NT
S.0048      DO 20 I=2,NX
S.0049      LA=NZ
S.0050      MA=M(I)-1
S.0051      SC1=1./(A1+X(I))*S2
S.0052      DO 24 J=LA,MA
S.0053      IF((DABS(Z(I,J))+DX)**2-(1.-X(I)**2))25,25,26
S.0054      25 CONTINUE
S.0055      IF((DABS(X(I))+DX)**2-(1.-Z(I,J)**2))27,27,26
CC 26 CALCULATION OF CONCENTRATION AT NODES WITH UNEQUAL INCREMENTS
S.0056      26 CONTINUE
S.0057      ALX=(DSQRT(DABS(1.-Z(I,J)**2))-DABS(X(I))+DX)/DX
S.0058      ALZ=(DSQRT(DABS(1.-X(I)**2))-DABS(Z(I,J))+DX)/DX
S.0059      IF(ALX-ALZ)28,28,29
S.0060      28 CONTINUE
S.0061      TH=(1.-ALX)
S.0062      GO TO 30
S.0063      29 CONTINUE
S.0064      TH=(1.-ALZ)
S.0065      GO TO 31
C 30 ALX LESS THAN ALZ
S.0066      30 CONTINUE
S.0067      IF(X(I)+0.0)62,62,63
C 62 X LESS THAN ZERO
S.0068      62 CONTINUE
S.0069      R(I,J)=(BC-(TH*((S+SC1)*C(I+2,J)+(S-SC1)*C(I,J)+S*C(I+1,J+1))+
/S*C(I+1,J-1)+(1.-4.*S)*C(I+1,J))))/ALX
S.0070      GO TO 39
C 63 X GREATER THAN ZERO
S.0071      63 CONTINUE
S.0072      R(I,J)=(BC-(TH*((S+SC1)*C(I,J)+(S-SC1)*C(I-2,J)+S*C(I-1,J+1))+
/S*C(I-1,J-1)+(1.-4.*S)*C(I-1,J))))/ALX
S.0073      GO TO 39

```

```

C      ALZ LESS THAN ALX
S.0074 31 CONTINUE
S.0075      R(I,J)=(RC-(TH*((S+SC1)*C(I+1,J-1)+(S-SC1)*C(I-1,J-1)+S*C(I,J)+
/ S*C(I,J-2)+(1.-4.*S)*C(I,J-1))))/ALZ
S.0076      GO TO 39
S.0077 27 CONTINUE
S.0078      IF(Z(I,J)+0.0)32,32,33
C      CALCULATION OF CONCENTRATION ALONG Z=0 LINE
S.0079 32 CONTINUE
S.0080      R(I,J)=(S+SC1)*C(I+1,J)+(S-SC1)*C(I-1,J)+2*S*C(I,J+1)+
/ (1.0-4.*S)*C(I,J)
S.0081      GO TO 39
C      CALCULATION OF CONCENTRATION AT EQUALLY SPACED POINTS
S.0082 33 CONTINUE
S.0083      R(I,J)=(S+SC1)*C(I+1,J)+(S-SC1)*C(I-1,J)+S*C(I,J+1)+S*C(I,J-1)+
/ (1.-4.*S)*C(I,J)
S.0084 39 CONTINUE
S.0085 24 CONTINUE
S.0086 20 CONTINUE
CCC     CALCULATION OF THE VOLUME AVERAGE CONCENTRATION
S.0087      DO 81 I=2,NX
S.0088      SUMF=0.0
S.0089      MA=M(I)-2
S.0090      LA=NZ
S.0091      IA=LA+1
S.0092      DO 85 J=IA,MA
S.0093      SUMF=SUMF+C(I,J)
S.0094 85 CONTINUE
S.0095      FXT(I)=DX*((C(I,LA)+C(I,MA+1))/2.+SUMF)+(Z(I,MA+2)-Z(I,MA+1))/2.
/ *(C(I,MA+1)+C(I,MA+2))
S.0096 81 CONTINUE
S.0097      STF=0.0
S.0098      DO 90 I=2,NX
S.0099      STF=STF+(A1+X(I))*FXT(I)
S.0100 90 CONTINUE
S.0101      CAV=R3*STF
S.0102      FF=1.0-CAV
S.0103      WRITE(2,100)TAU,C(37,1),FF,C(5,1)
CCC     COMPENSATION FOR LIMITED COMPUTER STORAGE
S.0104      DO 41 I=2,NX
S.0105      LA=N7
S.0106      MA=M(I)-1
S.0107      DO 46 J=LA,MA
S.0108      C(I,J)=R(I,J)
S.0109 46 CONTINUE
S.0110 41 CONTINUE
S.0111      TAU=DTA*KK
S.0112 70 CONTINUE
S.0113      CALL EXIT
S.0114      END

```



VIII. BIBLIOGRAPHY

- (1) Bird, R. B., Stewart, W. E. and Lightfoot, E. N., "Transport Phenomena", p. 555, John Wiley and Sons, New York (1960).
- (2) Crank, J., "The Mathematics of Diffusion", Oxford University Press, London (1956).
- (3) Fox, L., "Numerical Solution of Ordinary And Partial Differential Equations", p. 246, Addison-Wesley Company, Massachusetts (1962).
- (4) Handlos, A. E. and T. Baron, A. I. Ch. E. Journal, 3, 127 (1957).
- (5) Jacob B. Angelo, et al, A. I. Ch. E. Journal, 12 751 (1966).
- (6) Johns, L. E., Ph.D. Thesis, (1964), Carnegie Institute of Technology.
- (7) Kronig, R. and J. E. Brink, Applied Science Research, A-2, 142.
- (8) Newman, A. B., Trans. Am. Institute Chemical Engineers, 27, 203 (1931).
- (9) Richtonyer, R. D., "Difference Method For Initial Value Problems", Interscience Publishers Inc., New York (1957).
- (10) Rose, P. M. and R. C. Kintner, A. I. Ch. E. Journal 12, 530 (1966).
- (11) Saulyer, V. K., "International Series of Monographs In Pure and Applied Mathematics", Macmillan Company, New York (1964).
- (12) Taylor, A. E., "Advanced Calculus", p. 371, Ginn and Company, New York (1955).
- (13) Treybal, R. E., "Liquid Extraction", p. 470, McGraw-Hill Book Company, New York (1963).
- (14) Watson, G. N., "A Treatise on the Theory of Bessel Functions", p. 748, Macmillan Company, New York (1945).
- (15) Wellek, R. M. and A. H. P. Skelland, A. I. Ch. E. Journal, 11, 557 (1965).

IX. VITA

The author, Kamallesh Suryakant Desai, was born on April 27, 1944, in Parantij, India. He attended high school in Bombay and graduated in 1960. After high school, the author attended the University of Bombay and received the degree of Bachelor of Chemical Engineering in 1966. In September, 1966, he enrolled as a candidate for the Master of Science degree in Chemical Engineering at the University of Missouri at Rolla.